Journal of
Medicinal Chemistry

Article

Synthesis and Biological Evaluation of B-Cell Lymphoma 6 Inhibitors of N-phenyl-4-pyrimidinamine Derivatives Bearing Potent Activities against Tumor Growth.

Weikai Guo, Yajing Xing, qiansen zhang, Jiuqing Xie, Dongxia Huang, haijun Gu, peng he, Miaoran Zhou, Shifen Xu, Xiufeng Pang, Mingyao Liu, Zhengfang Yi, and Yihua Chen

J. Med. Chem., **Just Accepted Manuscript** • DOI: 10.1021/acs.jmedchem.9b01618 • Publication Date (Web): 02 Jan 2020

Just Accepted

is published by the American Chemical Society. 1155 Sixteenth Street N.W., Washington, DC 20036

Synthesis and Biological Evaluation of B-Cell Lymphoma 6 Inhibitors of *N*-Phenyl-4-pyrimidinamine Derivatives Bearing Potent Activities against Tumor Growth

Weikai Guo, [†,#] Yajing Xing, [†,#] Qiansen Zhang,[†] Jiuqing Xie,[†] Dongxia Huang,[†] Haijun Gu,[†] Peng He,[†] Miaoran Zhou,[‡] Shifen Xu,[‡] Xiufeng Pang,[†] Mingyao Liu,[†,] Zhengfang Yi,[†,*] Yihua Chen[†,*]*

[†]*East China Normal University and Shanghai Fengxian District Central Hospital Joint Center for Translational Medicine, Shanghai Key Laboratory of Regulatory Biology, Institute of Biomedical Sciences and School of Life Sciences, East China Normal University, 200241 Shanghai, China.*

[‡]*Shanghai University of Traditional Chinese Medicine, Shanghai, 200030, China*

ABSTRACT

The transcriptional repressor B-cell lymphoma 6 (BCL6) is frequently misregulated in diffuse large B-cell lymphoma (DLBCL) and has emerged as an attractive drug target for the treatments of lymphoma. In this article, a series of *N*-phenyl-4-pyrimidinamine derivatives were designed and synthesized as potent BCL6 inhibitors by optimizing hit

compound N^4-(3-chloro-4-methoxyphenyl)-N^2-isobutyl-5-fluoro-2,4-pyrimidinediamine on the basis of the structure-activity relationship. Among them, compound **14j** displayed the most potent activities, which significantly blocked the interaction of BCL6 with its corepressors, reactivated BCL6 target genes in a dose-dependent manner and had better effects compared with the two positive controls. Further studies indicated that a low dose of **14j** could effectively inhibit germinal center formation. More importantly, **14j** not only showed potent inhibition of DLBCL cell proliferation *in vitro* but also strongly suppressed the growth of DLBCL *in vivo*.

INTRODUCTION

B-cell lymphoma 6 (BCL6), as a transcriptional repressor and a member of the BTB/POZ/zinc finger family, was first identified as an oncogene in diffuse large B-cell lymphoma (DLBCL),[1-3] which is necessary for germinal center (GC) formation and T-cell dependent adaptive immune responses.[4, 5] BCL6 mediates a series of key cellular functions by repressing direct target genes mainly involved in the control of the cell cycle, gene transcription and DNA damage responses, among others.[6-8] Several lines of evidence suggest that DLBCL cells can be killed by delivering BCL6 shRNA, peptide inhibitors or small molecular inhibitors.[9-11] Most of the previous research results indicated that BCL6 was critical for the survival of DLBCL cells and could be a promising potential drug target for DLBCL therapy. In addition, BCL6 overexpression is found in many other tumors, which can induce lethality by targeting BCL6, such as breast cancer,[12-14] glioblastoma,[15, 16] ovarian cancer,[14, 17] and non–small cell lung cancer (NSCLC).[18] More importantly, BCL6 is also associated with drug resistance of tyrosine

kinase inhibitors (TKIs) in chronic myeloid leukemia (CML) cells and Ph-positive (Ph^+) acute lymphoblastic leukemia (ALL) cells.[19-21] For example, BCL6 is upregulated after treatments of TKIs in CML cells or Ph^+ ALL cells, which is required for a basic level of imatinib-resistance and CML stem cell survival as well as self-renewal in CML and Ph^+ ALL. Therefore, targeting BCL6 may also be a promising strategy to overcome resistance for TKI-treated CML and Ph^+ ALL. In addition, Dupont, T *et al*. have indicated that combination of BCL2 with BCL6 inhibitors may overcome the intrinsic resistance of BH3 mimetic inhibitors.[22]

The human proto-oncogene BCL6 encodes a 95-kDa protein,[4, 23, 24] which contains three regions: the N-terminal broad-complex/tramtrack/bric-a-brac (BTB) domain, a central unstructured region, and a set of six C-terminal zinc finger domains. The dimerization of the BCL6 BTB domain is necessary for its autonomous repressor activities, which can interact with three known corepressors, namely thyroid hormone receptors (SMRT),[4, 25-27] nuclear receptor corepressor (N-CoR) and BCL6 corepressor (B-CoR) in a mutually exclusive manner.[4, 25, 28] All three corepressors can bind to a commonly exposed surface at the interface of the two chains of the dimer, the lateral groove (LG).[27] Blocking the interaction of BCL6 with corepressors by mutation of the BCL6 BTB domain or BCL6 peptide inhibitors can inhibit GC formation and reactivate its target genes without any inflammation or other toxic effects.[8, 11, 27, 29, 30] The results indicate that the BCL6 BTB domain can be an excellent binding site for developing novel BCL6 inhibitors.

To date, several small molecular BCL6 inhibitors have been reported (Figure 1). For

example, compound **1** (**79-6**) was reported as the first small molecular BCL6 inhibitor that could bind to a pocket in the LG of the $BCL6^{BTB}$ domain with K_D of 138 μM.[31] Compound **2** (**FX1**), with a K_D of 7 μM, was obtained via subsequent structural modification of compound **1** by the same research group. Both of these proteins could disrupt BCL6 transcriptional complexes and reactivate BCL6 target genes. Moreover, compound **2** could disrupt GC formation, inhibit the proliferation of DLBCL cells *in vitro* and suppress the growth of DLBCL *in vivo* at a dose of 25 mg/kg/day.[32] However, compounds **1** and **2** with the same skeleton of rhodanine may be a detrimental, and they potentially have limitations for further drug development.[33, 34] Compound **3** could bind to the LG of the $BCL6^{BTB}$ homodimer and disrupt the interaction between BCL6 and the B-CoR peptide in a micromolar range.[35] Compound **4** could also bind to $BCL6^{BTB}$–LG in a nanomolar range.[36] Unfortunately, there are on reports further studies examing whether they could reactivate BCL6 target genes or inhibit GC formation, so it is not known whether these compounds could actually disrupt BCL6-mediated formation of repression complexes and translate into the de-repression of target genes. Compound **5** could bind to $BCL6^{BTB}$–LG and occupy the HDCH site with a K_D value of 44 μM, but it has not shown any antitumor growth effect, possibly due to its insufficient permeability.[33] Compound **6** (**BI-3802**) was reported to bind to $BCL6^{BTB}$ – LG and induce degradation of BCL6 in a nanomolar range as well as reactivate BCL6 target genes. Nevertheless, the functions of compound **6** have not been fully validated *in vivo* due to its poor bioavailability.[37] Therefore, the design and search for novel BCL6 inhibitors with better bioactivities both *in vitro* and *in vivo* remain a tremendous

challenge in this research field.

Based on our previous research work on diaminopyrimidine derivatives as anticancer agents,[38] we continuously modified this series of compounds and explored their anticancer potencies by studying whether they can interact with BCL6 given that most of the reported BCL6 inhibitors shared similar diaminopyrimidine scaffold. To discover more novel BCL6 inhibitors with high affinities, a preliminary screening program was initially carried out in our laboratory via the homogeneous time-resolved fluorescence (HTRF) assay. In brief, approximately 230 compounds containing diaminopyrimidine scaffold and other skeletons in in-house libraries were selected for screening at a concentration of 100 μM. Subsequently, 32 compounds with obvious inhibitory activities were screened at 50 μM. Finally, the active compounds were screened again at 25 μM. As a result, compound **7** (N^4-(3-chloro-4-methoxyphenyl)-N^2-isobutyl-5-fluoro-2,4-pyrimidinediamine) (Figure 2A) was identified, which could directly block BCL6 and SMRT interactions with an IC_{50} value of 19.4 ± 3.4 μM. In the present study, a series of novel *N*-phenyl-4-pyrimidinamine derivatives, with different amino-substitutions on hit **7**, were identified as potent BCL6 inhibitors through the elucidation of the structure−activity relationship. Among the investigated compounds, compound **14j** showed the best activities *in vitro* and *in vivo*, which was better than positive controls **2** and **3**. Compound **14j** significantly inhibited BCL6 and its corepressor interaction at low concentrations via direct binding to $BCL6^{BTB}$, and biological research subsequently showed that **14j** could also effectively reactivate BCL6 target genes in a dose-dependent manner. More importantly, compound **14j** significantly inhibited GC

formation and impaired immunoglobulin affinity maturation in mice at a low dose, in addition, it strongly suppressed the growth of DLBCL *in vivo*.

CHEMISTRY

Compounds **9a-n** were prepared in accordance with the procedures described in Scheme 1. 3-Chloro-4-methoxyaniline was coupled with 2,4-dichloro-5-fluoro-pyrimidine to afford key intermediate **8**. Then, **8** was substituted with various amines to obtain target compounds **9a-n**. Compounds **13a-f** were obtained via the following procedures listed in Scheme 2. The key intermediate **11a** was synthesized through similar procedures with compounds **9a-n**, and the only exception was to replace 3-chloro-4-methoxyaniline with 4-methoxy-3-nitroaniline. Compound **12a** was gained by the reduction of compound **11a**. Then, compounds **13a-f** were obtained by the coupling reaction of intermediate **12a** with various acids in the presence of EDC/HOBt or other coupling reagents.

Scheme 1[α]

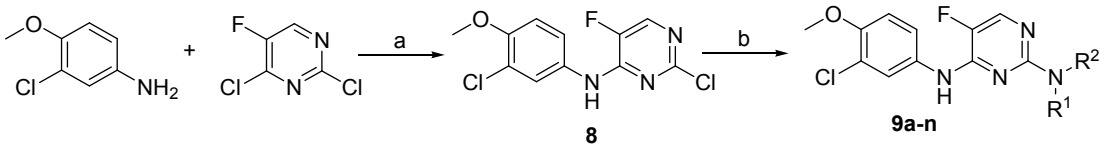

[α]Reagents and conditions: (a) DIEA, EtOH, 40 ℃; (b) R^1R^2NH, DIEA, *n*-BuOH, reflux.

Scheme 2[α]

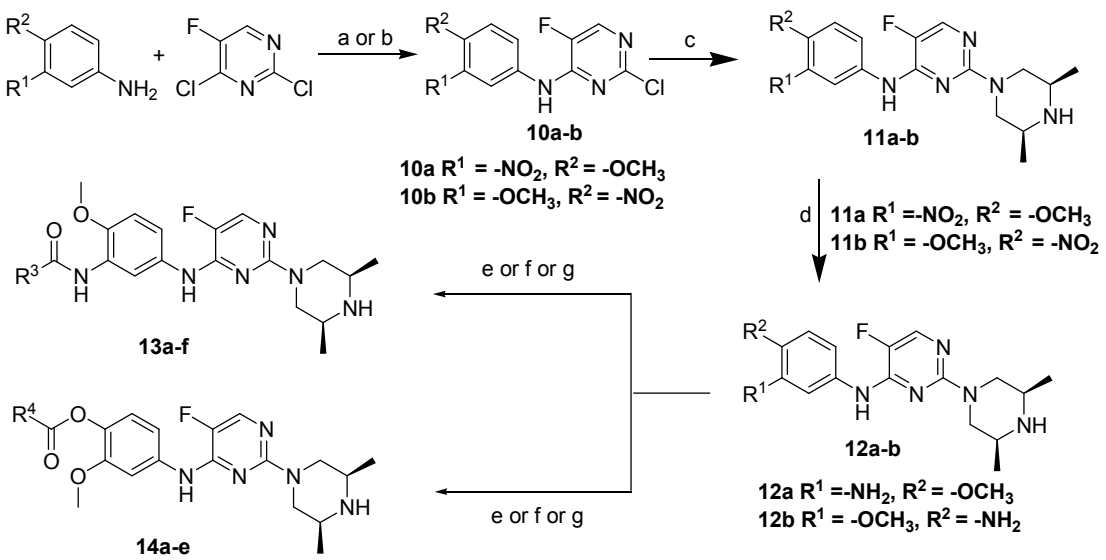

[α]Reagents and conditions: (a) DIEA, EtOH, 40 ℃; (b) Cs_2CO_3, DMF, r.t; (c) (2*S*,6*R*)-2,6-dimethylpiperazine, DIEA, *n*-BuOH, reflux; (d) Pd/C, H_2, MeOH; (e) EDC·HCl, HOBt, DMF, 0 ℃ then to r.t; (f) HATU, DMF, 0 ℃ then to r.t; (g) CDI, DMF, 0 ℃ then to r.t.

Compounds **14a-e** were prepared via a similar procedure as compounds **13a-f** (As shown in scheme 2), except for changing 4-methoxy-3-nitroaniline to 3-methoxy-4-nitroaniline. Compounds **14f-l** were synthesized according to the procedures described in Scheme 3 by Suzuki coupling reactions of methyl 5-bromothiophene-2-carboxylate with different boronic acids in the presence of $Pd(PPh_3)_4$ under the corresponding conditions, which were followed by acylation of the thiophene-2-carboxylic acid derivatives with compound **12b** to yield compounds **14f-l**.

Scheme 3[α]

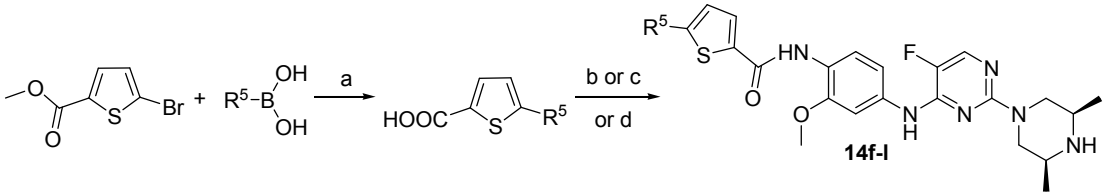

[α]Reagents and conditions:(a) $Pd(PPh_3)_4$, Na_2CO_3, EtOH, DME, 95 ℃; (b) EDC·HCl,

HOBt, DMF, 0 ℃ then to r.t; (c) HATU, DMF, 0 ℃ then to r.t; (d) CDI, DMF, 0 ℃ then to r.t.

RESULTS AND DISCUSSION

Structure activity relationship (SAR) analysis. The activities of target compounds to block the interaction of the co-repressor SMRT with the BTB domain of BCL6 were evaluated using the well-established HTRF assay. Compounds **2** and **3** were selected as the positive controls, and their IC_{50} values with BCL6 binding affinities were 37.7 ± 3.6 and 0.45 ± 0.1 μM, respectively, which were consistent with reported data.[35] In our preliminary data, compound **7** showed to mild inhibition with an IC_{50} of 19.4 ± 3.4 μM in the HTRF assay. Compound **7** shared a similar key scaffold to several reported BCL6 inhibitors, as shown in Figure 1, and it was selected as a hit and first modified with different amino-substitutions at the pyrimidine 2-position to increase the binding affinities. Compounds **9a−d** were first synthesized and then evaluated their IC_{50} values by HTRF assay (Table 1). The BCL6 inhibitory activities of ethylamine analogue **9a** and isopropylamine analogue **9b** were increased compared to that of **7** with IC_{50} values of 4.96 ± 0.8 and 4.83 ± 0.4 μM, respectively. However, substitutions with butylamine **9c** or diisobutylamine **9d** did not result in notable inhibitory effects (Table 1). To further increase the binding affinities of the target compounds, different tails of amino-alcohols and heterocyclic groups were introduced to the pyrimidinyl-2-position of compound **7**, and compounds **9e-n** were designed and synthesized (Table 1). Interestingly, the inhibitory activities of these compounds were greatly increased except for compounds **9i** and **9n**. Amino alcohol residues were superior to the corresponding substitutions of

aliphatic chain amines (**9e-g** *vs* **9a-d**). Furthermore, the substitution with propanolamine **9f** seemed to be more beneficial for inhibitory activity than ethanolamine **9e** or butanolamine **9g**. Substitutions with piperazine analogs (**9h**, **9j**, **9k** and **9m**) or morpholine analogue **9l** demonstrated significantly increased BCL6 inhibitory effects compared to hit **7**. Piperidine analogs (**9i** and **9n**) did not significantly inhibit the BCL6-SMRT interaction (Table 1). These results indicated that the existence of heteroatoms (such as NH or O) at the end of the substituents was preferred and critical for maintaining or increasing the inhibitory activities of the target compounds (**9h** *vs* **9i**, **9m** *vs* **9n**, **9e** *vs* **9a** and **9g** *vs* **9c**). Among them, compound **9h**, with (2*S*,6*R*)-2,6-dimethylpiperazinyl substitution, showed the best inhibitory activity, with an IC_{50} value of 0.77 ± 0.05 μM, which displayed comparable activity to positive control **3** and an activity level almost 45-fold higher than that of positive control **2** (Table 1).

Next, the substitutions in the left part of the phenyl ring of compound **9h** were investigated, and different substituents were introduced to the meta (*m*-) and para (*p*-) positions of the phenyl ring. First, the *m*-chloro atom of the phenyl ring was replaced with acyl residues, as shown in Figure 2B. Compounds **13a-f** were designed and synthesized (Table 2), and their IC_{50} values were tested via the HTRF assay. Unfortunately, all of these compounds greatly reduced or almost completely abolished BCL6 affinities compared with the effects of **9h**. The BCL6 inhibitory activities of bromophenyl analog **13c** and pyridyl analogs **13d-f** conferred weaker activities, whereas bromothienyl analogue **13a** and bromofuranyl analogue **13b** led to great loss in activities (IC_{50} > 20 μM). These results suggested that the introduction of acyl

residues to the *m*-position of the phenyl ring of **9h** were not conducive to improving BCL6 inhibitory activities.

Instead, our attention was next focused on the substitutions of the *p*-position of the left part of the phenyl ring of compound **9h** by changing its methoxy group from the *p*-position to the *m*-position (Figure 2B). To account for the efficacies of the target compounds containing acyl residues at this position interacting with $BCL6^{BTB}$, several docking simulations were conducted on the newly designed compounds to evaluate their potential interactions with the $BCL6^{BTB}$ domain (Figure 3). The high-resolution X-ray crystal structure of the $BCL6^{BTB}$ domain with the pyrazolo-pyrimidine macrocyclic ligand (PDB ID: 5N1Z) was used for docking simulations.[36] As shown in Figure 3A-C, the docking score of **14a**, which only exchanged the position of methoxy and acyl residues of compounds **13a** or **13c** between the *p*- and *m*-positions, was higher than that of **13a** and **13c**. To validate the prediction, compounds **14a-e** were synthesized by replacing the *m*-chlorine atom of the phenyl ring with *m*-methoxy, and introducing acyl residues at the corresponding position (Table 3). The BCL6 inhibitory activities of most of these compounds dramatically increased compared to the corresponding **13-series** derivatives (such as **14a** *vs* **13c** and **14c** *vs* **13f**), except for compounds **14b** and **14d** (Table 3). The results demonstrated that the introduction of acyl residues to the *p*-position of the phenyl ring was beneficial to improve the activities. Further modifications of substitutions at this position were explored and compounds **14f-l** were synthesized (Table 3). After converting the bromo atom of 5-bromothienyl of compound **14d** to phenyl (**14f-i**), cyclopentenyl (**14j**), cyclohexenyl (**14k**) or furanyl

(**14l**) via palladium-catalyzed coupling reactions, their potencies were increased to almost 10 to 20-fold compared to that of **14d** (Table 3). These results indicated that several cycloalkenyl-heteroaromatic or aryl-heteroaromatic groups were more suitable for enhancing inhibitory activities among the investigated compounds. Among these compounds, compound **14j** has the most potent activity with an IC_{50} of 0.47 ± 0.08 μM, with comparable activity to positive control **3** and was almost 80-fold more potent than the positive control **2** (Table 3).

To further elucidate how these potent compounds interacted with $BCL6^{BTB}$, compounds **14f**, **14j** and **14l**, which showed the highest activities among the tested compounds in the HTRF assay except for the above-mentioned compounds (**13a**, **13c** and **14a**), were also selected to conduct docking simulations. Before the docking simulations were carried out, quantum chemical calculations were performed on these new compounds in an attempt to provide molecular and electronic- based explanations for inhibitor binding (Figure S1). Quantum chemical calculations showed that the N atom on the piperazine ring has a negative charge and the H atom on N atom has a positive charge.

The docking results of **14a**, **14f**, **14j** and **14l** suggested that these compounds could bind to the $BCL6^{BTB}$ domain, and an analysis of the docking configurations reveals that these newly synthesized compounds assume similar binding models (Figure 3C-F). In the docking simulations, the N-H atom with a positive charge over the piperazine ring is bound to the non-protonated N atom in the residue His14 imidazole ring, which partly explains that the existence of a heteroatom in the terminal of the tail is preferred

in Table 1. The two nitrogen atoms from the pyrimidine ring interact with the side chain of N21 and H116 (Figure 3C-F). R24 is a relevant amino acid for the binding of compounds **14a**, **14f**, **14j** and **14l**, as its side chain interacts with the carbonyl oxygen of the acyl residues at the *p*-position of the phenyl ring on the left part of compounds (Figure 3C-F). Moreover, the annular segment located at the end group of compounds **14a**, **14f**, **14j** and **14l** can be stabilized by hydrophobic pockets formed by L25, M51 and Y58, among others (Figure 3C-F). Compared with these compounds, compounds **13a** and **13c**, containing acyl residues at the *m*-position of the phenyl ring, neither interact with R24 nor exert hydrophobic effects at the end group with the BCL6 ^{BTB} domain (Figure 3A-B). These docking results may partly explain why the activities of acyl residues introduced at the *p*-position of the phenyl ring on the left part of compounds are better than those of the corresponding analogs introduced at the *m*-position.

Compound 14j induces de-repression of BCL6 target genes in BCL6 dependent DLBCL cells. BCL6 mediates its biological effects by repressing its target genes, which are enriched in the modulators of the cell cycle, gene transcription, DNA damage responses and terminal plasma cell differentiation.[39] When knockdown of BCL6 is accomplished by delivering shRNA in two DLBCL cell lines (SUDHL4 and Farage), significant de-repression of BCL6 target genes (p53, ATR and CDKN1A) was observed compared with the control (Figure S2A-B). According to our above results with highly potent inhibition of BCL6, compounds **9h**, **14a**, **14j** and **14l** were selected to determine their abilities reactivate BCL6 target genes by real-time quantitative PCR assay in

SUDHL4 (a BCL6 dependent DLBCL cell line), and mRNA was collected after 24 h. The results showed that these compounds (5 μM) could significantly induce de-repression of BCL6 key target genes (ATR, CD69 and CXCR4) compared with the vehicle,[39] especially for **14j** (Figure S3). Since compound **14j** was the most active compound of reactivation of BCL6 target genes as well as possessed the best binding affinity of BCL6 among the investigated genes, two BCL6 dependent DLBCL cell lines (SUDHL4 and Farage) were further exposed to **14j** (5 μM), positive controls **2** (50 μM, as previously described[32]) and **3** (5 μM). The results showed that compound **14j** could significantly induce de-repression of BCL6 target genes (p53, ATR, CXCR4, CD69 and CDKN1A) compared with the vehicle,[39] which induced greater target gene reactivation compared with positive control **3** at the same concentration (5 μM) and positive control **2** even at a 10-fold concentration (50 μM) (Figure 4A). To further explore the selectivity of **14j**, two BCL6-dependent DLBCL cell lines (SUDHL4 and Farage) and a BCL6-independent DLBCL cell line (TOLEDO) were chosen to expose **14j** at concentrations of 1.25 μM, 2.50 μM and 5.00 μM, and mRNA was collected after 24 h. Compound **14j** resulted in an increase in the mRNA level of BCL6 target genes (p53, ATR, CDKN1A, CXCR4, CD69 and CD80) in a dose-dependent manner in the two BCL6-dependent DLBCL cell lines (Figure 4B). In sharp contrast to these phenomena, **14j** had little effect on any of these genes in the BCL6-independent DLBCL cell line (TOLEDO, Figure 4B). In general, these data indicated that **14j** could significantly and selectively reactivate BCL6 target genes in BCL6-dependent cancer cell lines in a dose-dependent manner.

Compound 14j binds the BCL6 BTB domain with potent affinity. Encouraged by these results, biolayer interferometry (BLI)[40, 41] was further chosen to study the kinetics of the BCL6 BTB domain binding affinity of compound **14j** on a ForteBIO Octet (Menlo Park, CA). Compounds **2** and **3** were also selected as the positive controls. As shown in Figure 5, compound **14j** could directly bind to the BCL6 BTB domain with a dissociation constant K_D value of 366 nM (Figure 5A), with a more than 20-fold greater affinity than positive control **2** (K_D of 7.88 μM), and a 3-fold greater affinity than positive control **3** (K_D of 1.19 μM) (Figure 5B-C).

Compound 14j significantly inhibits DLBCL growth *in vitro*. BCL6 favors the survival and proliferation of DLBCL. The loss of BCL6 function, which is mediated by delivering shRNA or BCL6 inhibitors, can kill DLBCL cells.[42] To verify the phenotype, DLBCL cells (SUDHL4 and Farage) were transfected with lentivirus expressing BCL6 shRNA and a nontargeted control shRNA. The results showed that BCL6 shRNA led to significantly reduced viabilities of DLBCL cells compared with the control (Figure S2A and S2C). Therefore, compound **14j** was further studied in a panel of four GCB-DLBCL cell lines (SUDHL-4, Farage, DOHH2 and OCI-LY7) and an ABC-DLBCL cell line (TOLEDO) to measure its antiproliferative effects via CCK8 assay for 72 h. The results are summarized in Table 4, and compounds **2** and **3** were selected as the positive controls. The results showed that compound **14j** displayed significant antiproliferative efficacies with average IC_{50} values of approximately 1 μM on four GCB-DLBCL cell lines, which was about 15 to 55-fold more potent than positive controls **2** and **3** (Table 4). TOLEDO was slightly less sensitive than the GCB-DLBCL

cell lines for compound **14j**, with an IC_{50} value of 3.25 μM, and TOLEDO cells responded to similar doses of positive controls **2** and **3**, which was consistent with previously reported results (Table 4),[32] and the knockdown of BCL6 by delivering shRNA was just as detrimental to ABC-DLBCL cells as to GCB-DLBCL cells.[32]

To further illustrate the relevance between the biological effects of **14j** and the function of BCL6, more experiments through knockdown or overexpression of BCL6 in different DLBCL cells were carried out to validate whether the inhibitory effects of **14j** on DLBCL cell growth were dependent or not by inhibiting the functions of BCL6. Farage cells with lentivirus expressing BCL6 shRNA were treated with **14j**. The results indicated that **14j** could effectively inhibit control vector cells in the investigated range of 0.5-2.0 μM in dose-dependent manner, while it showed little effect on BCL6 knockdown cells in the same concentration range (Figure S4A). However, positive controls **2** and **3** still showed similar antiproliferative effects against these DLBCL cells with or without knockdown of BCL6 (Figure S4A). In addition, we also transduced lentivirus overexpression of BCL6 in TOLEDO cells, showing an almost complete loss of BCL6 expression. The results demonstrated that **14j** had little effect against control vector cells in the range of 0.25-2.0 μM but showed significant antiproliferation against the DLBCL cell with overexpression of BCL6 in a dose-dependent manner at the same concentrations (Figure S4B). Compared to the effects observed with **14j**, positive control **2** showed weaker inhibition against this DLBCL cell with overexpression of BCL6, and **3** showed similar antiproliferative effects against these two DLBCL cells with or without overexpression of BCL6 in a range of 0-20 μM (Figure S4B),

supporting the notion that **14j** inhibits DLBCL cell growth by targeting BCL6. To subsequently evaluate the selectivity of **14j** against tumor cells, the cytotoxicities of compound **14j** were tested on four human normal cell lines (LO2, HAF, NCM460 and PNT1A), and the IC_{50} values of **14j** for DLBCL cells were approximately 20-fold lower than that of normal cells (Table 4), which demonstrated that **14j** results in specific levels of lethality on DLBCL cells.

One of the most accurate methods to measure cell proliferation is by directly measuring DNA synthesis. The EdU Flow Cytometry assay was conducted, which detects cell growth especially the cell population in the S phase. Treatment with compound **14j** for 48 h caused a sharp reduction in living cells in SUDHL4 cells in a dose-dependent manner, and fewer living cells and S phase cells were detected than in the counterparts of compounds **2** and **3** (Figure 6A). Previous studies showed that inhibition of BCL6 and its corepressor interaction by RI-BPI (a known BCL6 peptide inhibitor) or compound **2** led to DLBCL apoptosis.[11, 32] Compound **14j** was also selected to determine its effect on DLBCL apoptosis using flow cytometry. The results indicated that **14j** caused a dose-dependent induction of apoptosis at low doses of 0.625, 1.25 and 2.50 μM, while positive controls **2** and **3** did not induce apoptosis at the same concentrations (Figure 6B). Collectively, these results demonstrated that **14j** significantly inhibited DLBCL growth and induced apoptosis *in vitro*.

Compound 14j inhibits germinal center formation *in vivo*. The germinal center is a specialized structure that develops after T-cell-dependent antigen stimulation, where activated B cells proliferate, undergo somatic hyper-mutation, affinity maturation and

class-switch recombination, ultimately generating memory B cells and plasma cells that produce high-affinity antibodies.[43] The corepressors are unable to be recruited when there are mutations in the BCL6 BTB domain, which leads to the failure of GC formation and immunoglobulin affinity maturation in mice.[30] To identify whether compound **14j** could recapitulate this phenotype, we immunized C57/BL6 mice with 4-hydroxy-3-nitrophenylacetyl (NP)-coupled chicken gamma globulin (CGG), a T cell-dependent antigen. Two days later, compound **14j** with a 10 mg/kg/3d dose or vehicle was treated by tail intravenous injection (i.v.). A previous article reported that GC B cells were significantly depleted by exposure to compound **2**.[32] To verify the feasibility of the animal experiments, since compound **2** was not available with i.v. due to the limitation of its poor solubility, which was then given with a 50 mg/kg dose via intraperitoneal injection (i.p.) daily. Mice were euthanized and spleens were collected after 12 days of treatment with the compounds (when GCs are normally at their peak). As expected, GC B cells ($GL7^+FAS^+B220^+$) were significantly decreased by exposure to **14j** treatment group, which is similar to the BCL6 BTB domain mutant phenotype (Figure 7A). Compared with the control group, whose frequency of GC B cells was 1.97%, the group treated with **14j** exhibited better inhibitory activities against GC formation with a frequency of 0.45% (Figure 7A), and the compound **2** group exhibited a frequency of 0.73% (Figure S5A).

Splenic architecture was also examined by immunofluorescent staining. Staining with IgD antibody showed normal B cell follicular structures, and staining with peanut agglutinin (PNA) revealed GCs. Consistent with the results of the flow cytometry

analysis, both the number and size of GCs were decreased dramatically in the spleens of mice treated with compound **14j** compared with control mice (Figure 7B). Compound **2** also has an effect in impairing GC B cell development and GC formation (Figure S5B).

The development of Tfh cells in the germinal center was examined after treatment with compound **14j** since BCL6 was a crucial regulator of $CD4^+$ Tfh cell differentiation and maturation.[44] The results showed that the proportion of Tfh cells ($CXCR5^+PD1^+CD4^+$) was significantly depleted by exposure to the **14j** group (Figure 7C). Consistent with the better inhibitory activity of **14j** against the GCs, the proportion of Tfh cells was much lower in the **14j** group (0.99%) than in the control group (2.25%) (Figure 7C).

Recruitment of corepressors to the BTB domain was indispensable for BCL6 to drive the GC reaction to generate high-affinity immunoglobulins.[30] We determined whether compound **14j** could impair immunoglobulin affinity maturation by enzyme-linked immunosorbent assay (ELISA) (Figure 7D). As expected, compared to the control counterparts, mice treated with **14j** had much lower titers of high-affinity immunoglobulin G1 that was able to bind NP5-BSA (NP conjugated to bovine serum albumin (BSA) at a molecular ratio of 5:1), which recognizes high-affinity immunoglobulin (Figure 7D). This effect was also observed in the production of total NP-specific immunoglobulin G1 specific to NP23-BSA (NP conjugated to BSA at a molecular ratio of 23:1) (Figure 7D). Collectively, these results demonstrated that **14j** inhibited germinal center formation and impaired immunoglobulin affinity maturation.

Compound 14j potently suppresses BCL6 dependent DLBCLs *in vivo*. To further evaluate the anticancer efficacy of compound **14j** *in vivo*, we established an SCID DLBCL xenograft model using SUDHL4 DLBCL cells. When tumors reached a volume of approximately 100 mm^3, mice were randomly assigned to four groups (n = 7 per group) according to the dosing regimen: the control group (20% of (2-hydroxypropyl)-β-cyclodextrin by i.v.) and the **14j** treated groups (5 or 10 mg/kg/3d by i.v.). We also administered 25 mg/kg/d of compound **2** via i.p. as described to verify the feasibility of the animal experiments (Figure S6).[32] Animals were sacrificed when the control group reached the maximal permitted tumor burden. To our delight, compound **14j** significantly suppressed the tumor weight and volume even at the lower dosage (5 mg/kg/3d) compared with the control (Figure 8A-C). In addition, little difference was observed in body weight between **14j**-treated groups and control group (Figure 8D). Moreover, major organs including hearts, livers, spleens, lungs and kidneys were analyzed by H&E staining. No obvious damage to these organs was shown by H&E staining (Figure S7), which suggested that **14j** did not cause apparent adverse events with the treated doses. Ki67 staining was also explored in the tumors (Figure 8E). In comparison with the control, the expression of Ki67 was decreased prominently in the mice treated with **14j** (Figure 8E), which showed that **14j** significantly induced DLBCL cell growth arrest *in vivo*. To detect whether compound **14j** could de-repress BCL6 target genes *in vivo*, mRNA extracted from tumor tissue was evaluated for the abundance of BCL6 key target genes CD69, CXCR4 and ATR by real-time quantitative PCR (Figure 8F). Remarkably, **14j** significantly induced the

up-regulation of BCL6 target genes in DLBCL xenografts (Figure 8F). Taken together, these data underlined that **14j** potently suppressed BCL6 dependent DLBCLs *in vivo*.

Preliminary *in vitro* ADME study. Encouraged by these excellent biological results, compound **14j** was selected for a preliminary *in vitro* ADME assessment. As shown in Table 5, *in vitro* metabolism studies with human liver microsomes, revealed that compound **14j** exhibited low microsomal CL_{int} ($Cl_{int(mic)} < 9.6$ μL/min/mg and $Cl_{int(liver)} < 38.0$ mL/min/kg) and high metabolic stabilities ($T_{1/2} > 60$ min). The plasma protein binding (PPB) of humans was also measured. Excitingly, compound **14j** was also indicated modest plasma protein binding (7.6% free fraction).

CONCLUSION

BCL6 is necessary for GC formation and lymphomagenesis and has emerged as a critical therapeutic target in DLBCL. BCL6 mediates tumorigenesis via silencing its target genes. With knockdown of BCL6 by delivering shRNA, the BCL6 target genes were significantly reactivated and the DLBCL proliferation was obviously inhibited. Previous research results elucidated that BCL6 peptidomimetic inhibitor (RI-BPI) and small molecule inhibitors (**79-6** and **FX1**) can inhibit BCL6 and its corepressor interaction, resulting in de-repression of BCL6 target genes. More importantly, these BCL6 inhibitors can kill DLBCL cell lines as well as primary human DLBCL cells. All of these results demonstrated that BCL6 is important for the survival of DLBCL cells and that the antiproliferation effects of BCL6 inhibitors are largely due to the release from BCL6-mediated transcriptional repression. Therefore, one of the key factors inhibiting DLBCL proliferation by BCL6 inhibitors is to disrupt BCL6-mediated

formation of repression complexes and translate into de-repression of target genes.

In this study, a novel series of *N*-phenyl-4-pyrimidinamine derivatives were designed and optimized as potent BCL6 inhibitors based on the hit compound N^4-(3-chloro-4-methoxyphenyl)-N^2-isobutyl-5-fluoro-2,4-pyrimidinediamine **7**, which was identified to have mild BCL6 inhibition in the initial screening of a small-molecule library. Compound **14j**, as one of the most potent BCL6 inhibitors among the investigated compounds, could directly bind to the BCL6 BTB domain and significantly disrupt the BCL6-SMRT interaction. A real-time quantitative PCR assay showed that **14j** could specifically induce the de-repression of BCL6 target genes only in BCL6-dependent DLBCL cells with a dose-dependent manner. Further studies demonstrated that **14j** could significantly inhibit germinal center formation *in vivo*. Flow cytometry analysis and ELISA assay indicated that **14j** greatly reduced the proportion of Tfh cells and impaired immunoglobulin affinity maturation. More importantly, **14j** also strongly suppressed DLBCL growth *in vitro* and *in vivo*. In addition, we performed docking studies to simulate the binding mode of **14j** and $BCL6^{BTB}$. However, the exact binding mode of compound **14j** and $BCL6^{BTB}$ is unclear. Currently, we are trying to construct the mutant of $BCL6^{BTB}$ to identify the specific binding sites of compound **14j** to $BCL6^{BTB}$, these experiments are in progress.

Taken together, our results indicated that compound **14j** inhibited the proliferation of DLBCL *in vitro* and *in vivo* by directly binding to the $BCL6^{BTB}$ to block the interaction between BCL6 and SMRT and up-regulate BCL6 target genes. These new generations of *N*-phenyl-4-pyrimidinamine BCL6 inhibitors could be identified and

developed as novel potential anticancer agents against DLBCL growth in the future.

EXPERIMENTAL SECTION

General Methods for Chemistry. All commercially available reagents were purchased from bidepharm.com., Sigma-Aldrich Inc., J&K Inc., or Aladdin-Reagents Inc. and used without further purification. All reactions except those in H_2 atmosphere media were carried out with the use of standard techniques under an inert atmosphere (N_2). NMR spectra were generated on a Bruker 500 MHz instrument. High-resolution mass spectra were gathered on Bruker Micro-TOF-Q II LCMS instrument operating in electrospray ionization (ESI). High-pressure liquid chromatography (HPLC, Agilent Technologies 1200 Series) was conducted on an Eclipse XDB C18 column (5 μm, 4.6 mm × 150 mm) for purity determination, eluting with water (with 0.1% trifluoroacetic acid) and methanol (with 0.1% trifluoroacetic acid) at 40 °C for column temperature; gradient of 40-70% methanol (0-5 min), 70-90% methanol (5-15 min), 90-40% methanol (15-20 min) or 10-50% methanol (0-8 min), 50-90% methanol (8-15 min), 90-10% methanol (15-20 min) at the flow rate of 1.5 mL/min. All compounds purities were ≥ 95%, as verified by HPLC.

2-Chloro-*N*-(3-chloro-4-methoxyphenyl)-5-fluoro-4-pyrimidinamine (8). To a solution of 3-chloro-4-methoxyaniline (1.58 g, 10 mmol) and DIEA (5.2 mL, 30 mmol) in anhydrous EtOH (10 mL), then 2,4-dichloro-5-fluoropyrimidine (1.84 g, 11 mmol) was added, the mixture was stirred at 40 ℃ for overnight, the reaction mixture was concentrated under reduced pressure. The residue was partitioned between CH_2Cl_2 and

H_2O. The separated CH_2Cl_2 layer was washed with brine, dried over anhydrous Na_2SO_4 and evaporated to dryness, and then the residue was purified by column chromatography (eluting with PE/EA by 8:1-4:1) to give compound **8** (2.71 g, 94% yield). ^{1}H NMR (500 MHz, DMSO-d_6) δ 9.97 (s, 1H), 8.31 (d, J = 3.5 Hz, 1H), 7.78 (d, J = 2.6 Hz, 1H), 7.61 (dd, J = 9.0, 2.6 Hz, 1H), 7.19 (d, J = 9.0 Hz, 1H), 3.86 (s, 3H). HR MS (ESI): calcd for $C_{11}H_9Cl_2FN_3O$ $[M + H]^+$ 288.0101, found 288.0102.

***N*^{4}-(3-Chloro-4-methoxyphenyl)-*N*^{2}-ethyl-5-fluoro-2,4-pyrimidinediamine (9a)**. To a solution of intermediate **8** (144.1 mg, 0.5 mmol) and DIEA (0.26 mL, 1.5 mmol) in n-BuOH (5 mL), then ethylamine (0.32 mL, 5 mmol) was added, the mixture was stirred at 120 ℃ for overnight, the reaction mixture was concentrated under reduced pressure. The residue was partitioned between CH_2Cl_2 and H_2O. The separated CH_2Cl_2 layer was washed with brine, dried over anhydrous Na_2SO_4 and evaporated to dryness, and then the residue was purified by column chromatography (eluting with PE/EA by 4:1 followed by 100:1-20:1 CH_2Cl_2/MeOH) to give compound **9a** (115 mg, 77% yield). ^{1}H NMR (500 MHz, DMSO-d_6) δ 9.10 (s, 1H), 8.06 (s, 1H), 7.91 (d, J = 3.9 Hz, 1H), 7.69 – 7.68 (m, 1H), 7.09 (d, J = 9.0 Hz, 1H), 6.75 (s, 1H), 3.83 (s, 3H), 3.26 – 3.19 (m, 2H), 1.11 (t, J = 7.1 Hz, 3H). HPLC purity: 99.8%, R_t = 4.15 mim. HR MS (ESI): calcd for $C_{13}H_{15}ClFN_4O$ $[M + H]^+$ 297.0913, found 297.0918.

***N*^{4}-(3-Chloro-4-methoxyphenyl)-*N*^{2}-isopropyl-5-fluoro-2,4-pyrimidinediamine (9b)**. Compound **9b** (33% yield) was obtained through the similar synthetic route of compound **9a**, except replacing ethylamine with isopropylamine. ^{1}H NMR (500 MHz, DMSO-d_6) δ 9.09 (s, 1H), 8.05 (s, 1H), 7.91 (d, J = 3.8 Hz, 1H), 7.69 (d, J = 7.9 Hz,

1H), 7.09 (d, J = 9.0 Hz, 1H), 6.57 (d, J = 7.1 Hz, 1H), 3.90 – 3.89 (m,1H), 3.83 (s, 3H), 1.14 (d, J = 6.5 Hz, 6H). HPLC purity: 96.7%, R_t = 4.98 mim. HR MS (ESI): calcd for $C_{14}H_{17}ClFN_4O$ $[M + H]^+$ 311.1069, found 311.1073.

***N*⁴-(3-Chloro-4-methoxyphenyl)-*N*²-butyl-5-fluoro-2,4-pyrimidinediamine** (**9c**). Compound **9c** (94% yield) was obtained through the similar synthetic route of compound **9a**, except replacing ethylamine with butylamine. ^{1}H NMR (500 MHz, DMSO-d_6) δ 9.10 (s, 1H), 8.07 (s, 1H), 7.90 (d, J = 3.8 Hz, 1H), 7.67 (d, J = 6.1 Hz, 1H), 7.08 (d, J = 9.0 Hz, 1H), 6.77 (s, 1H), 3.82 (s, 3H), 3.21 – 3.17 (m, 2H), 1.54 – 1.45 (m, 2H), 1.38 – 1.28 (m, 2H), 0.88 (t, J = 7.3 Hz, 3H). HR MS (ESI): calcd for $C_{15}H_{19}ClFN_4O$ $[M + H]^+$ 325.1226, found 325.1228.

***N*⁴-(3-Chloro-4-methoxyphenyl)-*N*²,*N*²-diisobutyl-5-fluoro-2,4-pyrimidine-diamine** (**9d**). Compound **9d** (52% yield) was obtained through the similar synthetic route of compound **9a**, except replacing ethylamine with diisobutylamine. ^{1}H NMR (500 MHz, DMSO-d_6) δ 9.13 (s, 1H), 8.03 (d, J = 2.6 Hz, 1H), 7.97 (d, J = 3.8 Hz, 1H), 7.59 – 7.57 (m, 1H), 7.10 (d, J = 9.0 Hz, 1H), 3.83 (s, 3H), 3.32 – 3.31 (m, 4H), 2.13 – 2.03 (m, 2H), 0.84 (d, J = 6.7 Hz, 12H). HR MS (ESI): calcd for $C_{19}H_{27}ClFN_4O$ $[M + H]^+$ 381.1852, found 381.1857.

2-((4-((3-Chloro-4-methoxyphenyl)amino)-5-fluoro-2-pyrimidinyl)amino)-1-ethanol (9e). Compound **9e** (79% yield) was obtained through the similar synthetic route of compound **9a**, except replacing ethylamine with 2-aminoethanol. ^{1}H NMR (500 MHz, DMSO-d_6) δ 9.11 (s, 1H), 7.98 (s, 1H), 7.91 (d, J = 3.9 Hz, 1H), 7.72 – 7.71 (m, 1H), 7.09 (d, J = 9.0 Hz, 1H), 6.61 (t, J = 5.7 Hz, 1H), 4.63 (t, J = 5.4 Hz, 1H), 3.83

(s, 3H), 3.53 – 3.49 (m, 2H), 3.29 – 3.26 (m, 2H). HPLC purity: 97.7%, R_t = 7.83 mim. HR MS (ESI): calcd for $C_{13}H_{15}ClFN_4O_2$ $[M + H]^+$ 313.0862, found 313.0865.

3-((4-((3-Chloro-4-methoxyphenyl)amino)-5-fluoro-2-pyrimidinyl)amino)-1-propanol (9f). Compound **9f** (89% yield) was obtained through the similar synthetic route of compound **9a**, except replacing ethylamine with 3-aminopropanol. ^{1}H NMR (500 MHz, DMSO-d_6) δ 9.10 (s, 1H), 8.03 (s, 1H), 7.90 (d, J = 3.9 Hz, 1H), 7.72 – 7.70 (m, 1H), 7.09 (d, J = 9.0 Hz, 1H), 6.73 (s, 1H), 4.43 (t, J = 5.1 Hz, 1H), 3.83 (s, 3H), 3.47 (m, 2H), 3.25 – 3.24 (m, 2H), 1.71 – 1.63 (m, 2H). HPLC purity: 97.2%, R_t = 8.43 mim. HR MS (ESI): calcd for $C_{14}H_{17}ClFN_4O_2$ $[M + H]^+$ 327.1019, found 327.1019.

4-((4-((3-Chloro-4-methoxyphenyl)amino)-5-fluoro-2-pyrimidinyl)amino)-1-butanol (9g). Compound **9g** (85% yield) was obtained through the similar synthetic route of compound **9a**, except replacing ethylamine with 4-aminobutanol. ^{1}H NMR (500 MHz, DMSO-d_6) δ 9.10 (s, 1H), 8.06 (s, 1H), 7.90 (d, J = 3.9 Hz, 1H), 7.69 (d, J = 8.0 Hz, 1H), 7.09 (d, J = 9.0 Hz, 1H), 6.78 (s, 1H), 4.36 (t, J = 5.1 Hz, 1H), 3.83 (s, 3H), 3.40 (dd, J = 11.6, 6.3 Hz, 2H), 3.19 (dd, J = 13.1, 6.7 Hz, 2H), 1.57 – 1.50 (m, 2H), 1.49 – 1.43 (m, 2H). HPLC purity: 96.9%, R_t = 8.95 mim. HR MS (ESI): calcd for $C_{15}H_{19}ClFN_4O_2$ $[M + H]^+$ 341.1175, found 341.1178.

***N*-(3-Chloro-4-methoxyphenyl)-2-((3*S*,5*R*)-3,5-dimethyl-1-piperazinyl)-5-fluoro-4-pyrimidinamine (9h)**. Compound **9h** (79% yield) was obtained through the similar synthetic route of compound **9a**, except replacing ethylamine with (2*S*,6*R*)-2,6-dimethylpiperazine**.** ^{1}H NMR (500 MHz, DMSO-d_6) δ 9.28 (s, 1H), 8.11 (d, J = 2.6 Hz, 1H), 7.99 (d, J = 3.7 Hz, 1H), 7.51 – 7.49 (m, 1H), 7.13 (d, J = 9.0 Hz, 1H), 4.34 (d, J

= 11.8 Hz, 2H), 3.83 (s, 3H), 2.71 – 2.70 (m, 2H), 2.35 – 2.30 (m, 2H), 1.02 (d, J = 6.2 Hz, 6H). HPLC purity: 97.9%, R_t = 8.60 mim. HR MS (ESI): calcd for $C_{17}H_{22}ClFN_5O$ $[M + H]^+$ 366.1491, found 366.1495.

***N*-(3-Chloro-4-methoxyphenyl)-2-((3*R*,5*S*)-3,5-dimethyl-1-piperidinyl)-5-fluoro-4-pyrimidinamine (9i)**. Compound **9i** (87% yield) was obtained through the similar synthetic route of compound **9a**, except replacing ethylamine with (3*R*,5*S*)-3,5-dimethylpiperidine. ^{1}H NMR (500 MHz, DMSO-d_6) δ 9.24 (s, 1H), 8.11 (d, J = 2.4 Hz, 1H), 7.98 (d, J = 3.7 Hz, 1H), 7.50 (dd, J = 8.9, 2.5 Hz, 1H), 7.12 (d, J = 9.0 Hz, 1H), 4.48 (d, J = 11.8 Hz, 2H), 3.83 (s, 3H), 2.29 – 2.26 (m, 2H), 1.76 (d, J = 12.7 Hz, 1H), 1.58 – 1.47 (m, 2H), 0.89 (d, J = 6.5 Hz, 6H), 0.77 (d, J = 12.0 Hz, 1H). HR MS (ESI): calcd for $C_{18}H_{23}ClFN_4O$ $[M + H]^+$ 365.1539, found 365.1540.

***N*-(3-Chloro-4-methoxyphenyl)-5-fluoro-2-piperazinyl-4-pyrimidinamine (9j)**. Compound **9j** (98% yield) was obtained through the similar synthetic route of compound **9a**, except replacing ethylamine with piperazine. ^{1}H NMR (500 MHz, DMSO-d_6) δ 9.24 (s, 1H), 8.00 (d, J = 3.7 Hz, 1H), 7.91 (d, J = 2.6 Hz, 1H), 7.64 – 7.61 (m, 1H), 7.13 (d, J = 9.0 Hz, 1H), 5.76 (s, 1H), 3.83 (s, 3H), 3.58 – 3.49 (m, 4H), 2.77 – 2.67 (m, 4H). HPLC purity: 97.3%, R_t = 6.43 mim. HR MS (ESI): calcd for $C_{15}H_{18}ClFN_5O$ $[M + H]^+$ 338.1178, found 338.1179.

***N*-(3-Chloro-4-methoxyphenyl)-5-fluoro-2-(4-methyl-1-piperazinyl)-4-pyrimidinamine (9k)**. Compound **9k** (97% yield) was obtained through the similar synthetic route of compound **9a**, except replacing ethylamine with 1-methylpiperazine. ^{1}H NMR (500 MHz, DMSO-d_6) δ 9.27 (s, 1H), 8.00 (d, J = 3.6 Hz, 1H), 7.91 (d, J =

2.5 Hz, 1H), 7.62 – 7.61 (m, 1H), 7.13 (d, J = 9.0 Hz, 1H), 3.83 (s, 3H), 3.65 – 3.57 (m, 4H), 2.36 – 2.31 (m, 4H), 2.20 (s, 3H). HPLC purity: 98.9%, R_t = 6.54 mim. HR MS (ESI): calcd for $C_{16}H_{20}ClFN_5O$ $[M + H]^+$ 352.1335, found 352.1336.

***N*-(3-Chloro-4-methoxyphenyl)-5-fluoro-2-morpholino-4-pyrimidinamine (9l)**. Compound **9l** (91% yield) was obtained through the similar synthetic route compound **9a**, except replacing ethylamine with morpholine. ^{1}H NMR (500 MHz, DMSO-d_6) δ 9.30 (s, 1H), 8.03 (d, J = 3.7 Hz, 1H), 7.87 (d, J = 2.6 Hz, 1H), 7.67 – 7.62 (m, 1H), 7.13 (d, J = 9.0 Hz, 1H), 3.83 (s, 3H), 3.67 – 3.61 (m, 4H), 3.60 – 3.54 (m, 4H). HPLC purity: 98.0%, R_t = 9.11 mim. HR MS (ESI): calcd for $C_{15}H_{17}ClFN_4O_2$ $[M + H]^+$ 339.1019, found 339.1021.

***N*^{4}-(3-Chloro-4-methoxyphenyl)-5-fluoro-*N*^{2}-(1-methyl-4-piperidinyl)-2,4-pyrimidinediamine (9m)**. Compound **9m** (43% yield) was obtained through the similar synthetic route of compound **9a**, except replacing ethylamine with 1-methylpiperidin-4-amine. ^{1}H NMR (500 MHz, DMSO-d_6) δ 9.23 (s, 1H), 7.98 (d, J = 3.6 Hz, 1H), 7.97 (d, J = 2.4 Hz, 1H), 7.58 – 7.57 (m, 1H), 7.12 (d, J = 9.0 Hz, 1H), 4.33 (d, J = 13.2 Hz, 2H), 4.12 – 4.05 (m, 1H), 3.83 (s, 3H), 3.32 (s, 3H), 2.96 – 2.91 (m, 2H), 2.83 – 2.78 (m, 1H), 1.73 – 1.70 (m, 2H), 1.19 – 1.12 (m, 2H). HPLC purity: 96.1%, R_t = 6.41 mim. HR MS (ESI): calcd for $C_{17}H_{22}ClFN_5O$ $[M + H]^+$ 366.1491, found 366.1493.

***N*^{4}-(3-Chloro-4-methoxyphenyl)-*N*^{2}-cyclohexyl-5-fluoro-2,4-pyrimidinediamine (9n)**. Compound **9n** (98% yield) was obtained through the similar synthetic route of compound **9a**, except replacing ethylamine with cyclohexanamine.

^{1}H NMR (500 MHz, DMSO-d_6) δ 9.09 (s, 1H), 8.08 (s, 1H), 7.90 (d, J = 3.8 Hz, 1H), 7.65 (s, 1H), 7.08 (d, J = 9.0 Hz, 1H), 6.60 (d, J = 4.7 Hz, 1H), 3.83 (s, 3H), 2.09 (s, 1H), 1.89 (d, J = 10.7 Hz, 2H), 1.71 (d, J = 12.9 Hz, 2H), 1.60 (d, J = 12.7 Hz, 1H), 1.31 – 1.30 (m, 2H), 1.25 – 1.18 (m, 2H), 1.15 – 1.06 (m, 1H). HPLC purity: 98.7%, R_t = 6.73 mim. HR MS (ESI): calcd for $C_{17}H_{21}ClFN_4O$ $[M + H]^+$ 351.1382, found 351.1384.

2-Chloro-5-fluoro-*N*-(4-methoxy-3-nitrophenyl)-4-pyrimidinamine (10a). Compound **10a** was obtained through the similar synthetic route of compound **8**, except replacing 3-chloro-4-methoxyaniline with 4-methoxy-3-nitroaniline (91% yield). ^{1}H NMR (500 MHz, DMSO-d_6) δ 10.18 (s, 1H), 8.36 (d, J = 3.4 Hz, 1H), 8.27 (d, J = 2.7 Hz, 1H), 7.96 (dd, J = 9.1, 2.7 Hz, 1H), 7.44 (d, J = 9.2 Hz, 1H), 3.94 (s, 3H). HR MS (ESI): calcd for $C_{11}H_8ClFN_4NaO_3$ $[M + H]^+$ 321.0161, found 321.0165.

2-Chloro-5-fluoro-*N*-(3-methoxy-4-nitrophenyl)-4-pyrimidinamine (10b). To a solution of 3-methoxy-4-nitroaniline (840.8 mg, 5.0 mmol) and Cs_2CO_3 (4.882 g, 15.0 mmol) in anhydrous DMF (5 mL), then 2,4-dichloro-5-fluoropyrimidine (1.67 g, 10.0 mmol) was added, the mixture was stirred at r.t for overnight. The residue was partitioned between CH_2Cl_2 and H_2O. The separated CH_2Cl_2 layer was washed with brine, dried over anhydrous Na_2SO_4 and evaporated to dryness, and then the residue was purified by column chromatography (eluting with PE/EA by 8:1-4:1) to give compound **10b** (725.0 mg, 49% yield). ^{1}H NMR (500 MHz, DMSO-d_6) δ 8.95 (s, 1H), 8.94 (s, 1H), 7.99 (d, J = 8.7 Hz, 1H), 7.53 (d, J = 1.6 Hz, 1H), 7.24 (dd, J = 8.7, 1.9 Hz, 1H), 3.85 (s, 3H). HR MS (ESI): calcd for $C_{11}H_8ClFN_4NaO_3$ $[M + H]^+$ 321.0161,

found 321.0157.

2-((3*S*,5*R*)-3,5-Dimethyl-1-piperazinyl)-5-fluoro-*N*-(4-methoxy-3-nitrophenyl)-4-pyrimidinamine (11a). Compound **11a** (83% yield) was obtained through the similar synthetic route of compound **9a**, except replacing compound **8** with compound **10a** instead of and replacing ethylamine with (2*S*,6*R*)-2,6-dimethylpiperazine. ^{1}H NMR (500 MHz, DMSO-d_6) δ 9.51 (s, 1H), 8.72 (d, J = 2.7 Hz, 1H), 8.03 (d, J = 3.6 Hz, 1H), 7.78 (dd, J = 9.1, 2.7 Hz, 1H), 7.37 (d, J = 9.2 Hz, 1H), 4.37 (d, J = 11.0 Hz, 2H), 3.91 (s, 3H), 2.71 – 2.69 (m, 2H), 2.32 – 2.30 (m, 2H), 1.02 (d, J = 6.2 Hz, 6H). HR MS (ESI): calcd for $C_{17}H_{22}FN_6O_3$ $[M + H]^+$ 377.1732, found 377.1737.

2-((3*S*,5*R*)-3,5-Dimethyl-1-piperazinyl)-5-fluoro-*N*-(3-methoxy-4-nitrophenyl)-4-pyrimidinamine (11b). Compound **11b** (86% yield) was obtained through the similar synthetic route of compound **11a**, except replacing compound **10a** with compound **10b**. ^{1}H NMR (500 MHz, DMSO-d_6) δ 9.77 (s, 1H), 8.16 (d, J = 3.4 Hz, 1H), 7.98 (dd, J = 5.5, 3.5 Hz, 2H), 7.43 (dd, J = 9.1, 2.1 Hz, 1H), 4.37 (d, J = 10.5 Hz, 2H), 3.94 (s, 3H), 2.71 – 2.67 (m, 2H), 2.36 – 2.31 (m, 2H), 1.00 (d, J = 6.2 Hz, 6H). HR MS (ESI): calcd for $C_{17}H_{22}FN_6O_3$ $[M + H]^+$ 377.1732, found 377.1730.

***N*^{1}-(2-((3*S*,5*R*)-3,5-Dimethyl-1-piperazinyl)-5-fluoro-4-pyrimidinyl)-4-methoxy-benzene-1,3-diamine (12a)**. To a solution of compound **11a** (1.694 g, 4.5 mmol) in anhydrous MeOH (50 mL) was added Pd-C under N_2. The suspension was degassed under vacuum and purged with H_2 several times. The mixture was stirred under H_2 at r.t for overnight. The suspension was filtered and the filtrate was concentrated by rotary evaporation to give compound **12a** (95%). ^{1}H NMR (500 MHz, DMSO-d_6) δ 8.87 (s,

1H), 7.91 (d, *J* = 3.9 Hz, 1H), 7.00 (d, *J* = 2.5 Hz, 1H), 6.87 (dd, *J* = 8.6, 2.5 Hz, 1H), 6.73 (d, *J* = 8.7 Hz, 1H), 4.69 (s, 2H), 4.38 (d, *J* = 10.9 Hz, 2H), 3.74 (s, 3H), 2.77 – 2.75 (m, 2H), 2.35 – 2.33 (m, 2H), 1.03 (d, *J* = 6.2 Hz, 6H). HR MS (ESI): calcd for $C_{17}H_{24}FN_6O$ $[M + H]^+$ 347.1990, found 347.1993.

***N*^{1}-(2-((3*S*,5*R*)-3,5-Dimethyl-1-piperazinyl)-5-fluoro-4-pyrimidinyl)-3-methoxy -benzene-1,4-diamine (12b)**. Compound **12b** (90% yield) was obtained through the similar synthetic route of compound **12a**, except replacing compound **11a** with compound **11b**. ^{1}H NMR (500 MHz, DMSO-d_6) δ 9.08 (s, 1H), 7.97 (d, *J* = 3.5 Hz, 1H), 7.27 (d, *J* = 1.5 Hz, 1H), 6.95 (dd, *J* = 8.4, 1.7 Hz, 1H), 6.58 (d, *J* = 8.3 Hz, 1H), 4.59 (d, *J* = 0.5 Hz, 2H), 3.76 (s, 3H), 3.30 – 3.22 (m, 2H), 2.82 – 2.77 (m, 2H), 1.24 (d, *J* = 6.3 Hz, 7H). HR MS (ESI): calcd for $C_{17}H_{24}FN_6O$ $[M + H]^+$ 347.1990, found 347.1991.

5-Bromo-*N*-(5-((2-((3*S*,5*R*)-3,5-dimethyl-1-piperazinyl)-5-fluoro-4-pyrimidinyl) amino)-2-methoxyphenyl)thiophene-2-carboxamide (13a). A mixture of compound 5-bromothiophene-2-carboxylic acid (155.3 mg, 0.75 mmol) in anhydrous DMF (2 mL) were added EDC·HCl (125.0 mg, 1.3 mmol) and HOBt (74.0 mg, 1.1 mmol) at 0 ℃, and then compound **12a** (173.2 mg, 0.5 mmol) was added to the mixture after stirring for 15 min. The mixture was stirred at r.t for overnight, the reaction mixture was concentrated under reduced pressure. The residue was partitioned between CH_2Cl_2 and H_2O. The separated CH_2Cl_2 layer was washed with brine, dried over anhydrous Na_2SO_4 and evaporated to dryness, and concentrated, and then the residue was purified by column chromatography (eluting with CH_2Cl_2/MeOH by 100:1-20:1) to give

compound **13a** (148 mg, 55% yield). ^{1}H NMR (500 MHz, DMSO-d_6) δ 9.66 (s, 1H), 9.30 (s, 1H), 8.33 (d, J = 2.4 Hz, 1H), 8.02 (d, J = 3.6 Hz, 1H), 7.88 (d, J = 4.0 Hz, 1H), 7.36 (d, J = 4.0 Hz, 1H), 7.31 – 7.30 (m, 1H), 7.08 (d, J = 9.0 Hz, 1H), 4.59 (d, J = 13.3 Hz, 2H), 3.83 (s, 3H), 3.17 – 3.16 (m, 2H), 2.74 – 2.69 (m, 2H), 1.19 (d, J = 6.2 Hz, 7H). HR MS (ESI): calcd for $C_{22}H_{25}BrFN_6O_2S$ $[M + H]^+$ 535.0922, found 535.0923.

5-Bromo-*N*-(5-((2-((3*S*,5*R*)-3,5-dimethyl-1-piperazinyl)-5-fluoro-4-pyrimidinyl) amino)-2-methoxyphenyl)furan-2-carboxamide (13b). Compound **13b** (90% yield) was obtained through the similar synthetic route of compound **13a**, except replacing 5-bromothiophene-2-carboxylic acid with 5-bromofuran-2-carboxylic acid. ^{1}H NMR (500 MHz, DMSO-d_6) δ 9.27 (s, 1H), 9.21 (s, 1H), 8.50 (d, J = 2.6 Hz, 1H), 7.98 (d, J = 3.7 Hz, 1H), 7.34 (d, J = 3.6 Hz, 1H), 7.07 (d, J = 9.0 Hz, 1H), 6.84 (d, J = 3.6 Hz, 1H), 4.43 (d, J = 11.9 Hz, 2H), 3.85 (s, 3H), 2.81 – 2.80 (m, 2H), 2.38 – 2.34 (m, 2H), 1.00 (d, J = 5.9 Hz, 6H). HR MS (ESI): calcd for $C_{22}H_{25}BrFN_6O_3$ $[M + H]^+$ 519.1150, found 519.1153.

3-Bromo-*N*-(5-((2-((3*S*,5*R*)-3,5-dimethyl-1-piperazinyl)-5-fluoro-4-pyrimidinyl) amino)-2-methoxyphenyl)benzamide (13c). Compound **13c** (50% yield) was obtained through the similar synthetic route of compound **13a**, except replacing 5-bromothiophene-2-carboxylic acid with 3-bromobenzoic acid. ^{1}H NMR (500 MHz, DMSO-d_6) δ 9.65 (s, 1H), 9.34 (s, 2H), 8.43 (s, 1H), 8.14 (s, 1H), 8.04 (s, 1H), 7.96 (d, J = 7.1 Hz, 1H), 7.82 (d, J = 7.3 Hz, 1H), 7.51 (t, J = 7.5 Hz, 1H), 7.31 (d, J = 8.1 Hz, 1H), 7.09 (d, J = 8.8 Hz, 1H), 4.63 (d, J = 13.1 Hz, 2H), 3.84 (s, 3H), 3.26 – 3.24 (m, 2H), 2.83 – 2.78 (m, 2H), 1.21 (d, J = 3.6 Hz, 6H). HPLC purity: 99.3%, R_t = 4.59 mim.

HR MS (ESI): calcd for $C_{24}H_{27}BrFN_6O_2$ $[M + H]^+$ 529.1357, found 529.1359.

***N*-(5-((2-((3*S*,5*R*)-3,5-Dimethyl-1-piperazinyl)-5-fluoro-4-pyrimidinyl)amino)-2-methoxyphenyl)picolinamide (13d)**. Compound **13d** (38% yield) was obtained through the similar synthetic route of compound **13a**, except replacing 5-bromothiophene-2-carboxylic acid with picolinic acid instead of. ^{1}H NMR (500 MHz, DMSO-d_6) δ 10.54 (s, 1H), 9.54 (d, J = 9.6 Hz, 1H), 9.16 (d, J = 2.5 Hz, 1H), 8.99 (d, J = 8.5 Hz, 1H), 8.77 (d, J = 4.5 Hz, 1H), 8.13 – 8.12 (m, 1H), 7.74 – 7.71 (m, 1H), 7.23 – 7.22 (m, 1H), 7.13 (d, J = 8.9 Hz, 1H), 4.69 (d, J = 12.6 Hz, 2H), 3.95 (s, 3H), 3.33 – 3.30 (m, 2H), 2.94 – 2.85 (m, 2H), 1.22 (d, J = 5.2 Hz, 6H). HPLC purity: 98.1%, R_t = 6.89 mim. HR MS (ESI): calcd for $C_{23}H_{27}FN_7O_2$ $[M + H]^+$ 452.2205, found 452.2211.

6-Fluoro-*N*-(5-((2-((3*S*,5*R*)-3,5-dimethyl-1-piperazinyl)-5-fluoro-4-pyrimidinyl) amino)-2-methoxyphenyl)picolinamide (13e). Compound **13e** (71% yield) was obtained through the similar synthetic route of compound **13a**, except replacing 5-bromothiophene-2-carboxylic acid with 6-fluoropicolinic acid. ^{1}H NMR (500 MHz, DMSO-d_6) δ 10.11 (s, 1H), 9.74 (s, 1H), 9.07 (d, J = 2.4 Hz, 1H), 8.33 (dd, J = 15.6, 7.9 Hz, 1H), 8.13 (d, J = 4.1 Hz, 1H), 8.10 (dd, J = 7.4, 1.8 Hz, 1H), 7.57 (dd, J = 8.2, 1.5 Hz, 1H), 7.28 (dd, J = 8.9, 2.6 Hz, 1H), 7.16 (d, J = 8.9 Hz, 1H), 4.67 (d, J = 12.1 Hz, 2H), 3.96 (s, 3H), 3.36 – 3.27 (m, 2H), 2.99 – 2.95 (m, 2H), 1.24 (d, J = 6.3 Hz, 6H). HR MS (ESI): calcd for $C_{23}H_{26}F_2N_7O_2$ $[M + H]^+$ 470.2111, found 470.2121.

6-Bromo-*N*-(5-((2-((3*S*,5*R*)-3,5-dimethyl-1-piperazinyl)-5-fluoro-4-pyrimidinyl) amino)-2-methoxyphenyl)picolinamide (13f). Compound **13f** (33% yield) was

obtained through the similar synthetic route of compound **13a**, except replacing 5-bromothiophene-2-carboxylic acid with 6-bromopicolinic acid. ^{1}H NMR (500 MHz, DMSO-d_6) δ 10.21 (s, 1H), 9.37 (s, 1H), 9.10 (d, J = 2.4 Hz, 1H), 8.15 (d, J = 7.5 Hz, 1H), 8.08 (t, J = 7.7 Hz, 1H), 8.05 (d, J = 3.6 Hz, 1H), 7.99 (d, J = 7.8 Hz, 1H), 7.25 (dd, J = 8.9, 2.5 Hz, 1H), 7.14 (d, J = 8.9 Hz, 1H), 4.70 (d, J = 12.1 Hz, 2H), 3.94 (s, 3H), 3.30 – 3.26 (m, 2H), 2.84 – 2.77 (m, 2H), 1.22 (d, J = 6.2 Hz, 6H). HR MS (ESI): calcd for $C_{23}H_{26}BrFN_7O_2$ $[M + H]^+$ 530.1310, found 530.1316.

3-Bromo-*N*-(4-((2-((3*S*,5*R*)-3,5-dimethyl-1-piperazinyl)-5-fluoro-4-pyrimidinyl) amino)-2-methoxyphenyl)benzamide (14a). Compound **14a** (57% yield) was obtained through the similar synthetic route of compound **13c**, except replacing compound **12a** with compound **12b**. ^{1}H NMR (500 MHz, DMSO-d_6) δ 9.65 (s, 1H), 9.44 (s, 1H), 8.12 (d, J = 20.7 Hz, 2H), 7.96 (d, J = 3.6 Hz, 1H), 7.79 (d, J = 5.5 Hz, 1H), 7.62 (s, 1H), 7.55 (s, 1H), 7.49 (s, 1H), 7.31 (d, J = 6.3 Hz, 1H), 4.60 (d, J = 12.9 Hz, 2H), 3.83 (s, 3H), 3.30 – 3.20 (m, 2H), 2.99 – 2.83 (m, 2H), 1.29 (d, J = 6.2 Hz, 6H). HPLC purity: 97.8%, R_t = 4.88 mim. HR MS (ESI): calcd for $C_{24}H_{27}BrFN_6O_2$ $[M + H]^+$ 529.1357, found 529.1362.

5-Bromo-*N*-(4-((2-((3*S*,5*R*)-3,5-dimethyl-1-piperazinyl)-5-fluoro-4-pyrimidinyl) amino)-2-methoxyphenyl)furan-2-carboxamide (14b). Compound **14b** (30% yield) was obtained through the similar synthetic route of compound **14a**, except replacing 3-bromobenzoic acid with 5-bromofuran-2-carboxylic. ^{1}H NMR (500 MHz, DMSO-d_6) δ 9.40 (s, 1H), 9.30 (s, 1H), 8.08 (d, J = 1.9 Hz, 1H), 7.64 (d, J = 5.9 Hz, 1H), 7.62 (s, 1H), 7.34 (s, 1H), 7.29 (d, J = 8.5 Hz, 1H), 6.83 (d, J = 3.3 Hz, 1H), 4.54 (d, J = 13.0

Hz, 2H), 3.85 (s, 3H), 3.14 – 3.12 (m, 2H), 2.73 – 2.66 (m, 2H), 1.19 (d, J = 4.8 Hz, 6H). HR MS (ESI): calcd for $C_{22}H_{25}BrFN_6O_3$ $[M + H]^+$ 519.1150, found 519.1155.

6-Bromo-*N*-(4-((2-((3*S*,5*R*)-3,5-dimethyl-1-piperazinyl)-5-fluoro-4-pyrimidinyl) amino)-2-methoxyphenyl)picolinamide (14c). Compound **14c** (42% yield) was obtained through the similar synthetic route of compound **14a**, except replacing 3-bromobenzoic acid with 6-bromopicolinic acid. ^{1}H NMR (500 MHz, DMSO-d_6) δ 10.06 (s, 1H), 9.44 (s, 1H), 8.29 (d, J = 8.8 Hz, 1H), 8.18 (d, J = 7.5 Hz, 1H), 8.09 (d, J = 3.5 Hz, 1H), 8.04 (t, J = 7.7 Hz, 1H), 7.96 (d, J = 7.9 Hz, 1H), 7.68 (d, J = 2.1 Hz, 1H), 7.35 – 7.34 (m, 1H), 4.58 (d, J = 13.4 Hz, 2H), 3.95 (s, 3H), 3.22 – 3.21 (m, 2H), 2.86 – 2.81 (m, 2H), 1.26 (d, J = 6.4 Hz, 6H). HPLC purity: 100%, R_t = 5.50 mim.HR MS (ESI): calcd for $C_{23}H_{26}BrFN_7O_2$ $[M + H]^+$ 530.1310, found 530.1317.

5-Bromo-*N*-(4-((2-((3*S*,5*R*)-3,5-dimethyl-1-piperazinyl)-5-fluoro-4-pyrimidinyl) amino)-2-methoxyphenyl)thiophene-2-carboxamide (14d). Compound **14d** (43% yield) was obtained through the similar synthetic route of compound **14a**, except replacing 3-bromobenzoic acid with 5-bromothiophene-2-carboxylic acid. ^{1}H NMR (500 MHz, DMSO-d_6) δ 9.67 (s, 1H), 9.45 (s, 1H), 8.92 (d, J = 2.2 Hz, 1H), 8.10 (d, J = 2.2 Hz, 1H), 7.85 (d, J = 4.5 Hz, 1H), 7.60 (s, 1H), 7.47 (d, J = 7.3 Hz, 1H), 7.34 (s, 1H), 4.60 (d, J = 13.4 Hz, 2H), 3.83 (s, 3H), 3.20 – 3.16 (m, 2H), 2.92 – 2.85 (m, 2H), 1.27 (d, J = 3.0 Hz, 6H). HR MS (ESI): calcd for $C_{22}H_{25}BrFN_6O_2S$ $[M + H]^+$ 535.0922, found 535.0923.

***N*-(4-((2-((3*S*,5*R*)-3,5-Dimethyl-1-piperazinyl)-5-fluoro-4-pyrimidinyl)amino)-2-methoxyphenyl)benzo[b]thiophene-2-carboxamide (14e)**. Compound **14e** (67%

yield) was obtained through the similar synthetic route of compound **14a**, except replacing 3-bromobenzoic acid with benzo[b]thiophene-2-carboxylic acid. ^{1}H NMR (500 MHz, DMSO-d_6) δ 9.80 (s, 1H), 9.47 (s, 1H), 8.35 (s, 1H), 8.11 (d, J = 3.5 Hz, 1H), 8.05 (d, J = 7.5 Hz, 1H), 7.99 (d, J = 7.0 Hz, 1H), 7.64 (d, J = 2.0 Hz, 1H), 7.60 (d, J = 8.6 Hz, 1H), 7.52 – 7.40 (m, 2H), 7.34 (dd, J = 8.6, 2.0 Hz, 1H), 4.61 (d, J = 12.4 Hz, 2H), 3.86 (s, 3H), 3.30 – 3.26 (m, 2H), 2.96 – 2.84 (m, 2H), 1.29 (d, J = 6.4 Hz, 6H). HPLC purity: 99.9%, R_t = 5.32 mim. HR MS (ESI): calcd for $C_{26}H_{28}FN_6O_2S$ $[M + H]^+$ 507.1973, found 507.1976.

***N*-(4-((2-((3*S*,5*R*)-3,5-Dimethyl-1-piperazinyl)-5-fluoro-4-pyrimidinyl)amino)-2-methoxyphenyl)-5-phenylthiophene-2-carboxamide (14f)**. Step 1: To a solution of compound methyl 5-bromothiophene-2-carboxylate (221 mg, 1.0 mmol) was dissolved in 1,2-dimethoxyethane (2.5 mL) and anhydrous ethanol (4 mL), catalytic tetrakis(triphenylphosphine)palladium was added at r.t, and then the vial was purged with nitrogen and stirred for 5 min. Subsequently, phenylboronic acid (244 mg, 2.0 mmol) and aqueous solution of Na_2CO_3 (2.0 mol/L, 5 mL) were added to the mixture, the vial was purged with nitrogen again, and the resulting mixture was heated to 95 ℃ for overnight. After the reaction was complete, the reaction mixture was concentrated under reduced pressure and then 50 mL of ice-water carefully was poured and the aqueous phase was washed with CH_2Cl_2 (100 mL) and acidified with 1N HCl to pH = 1. The resulting precipitate was collected by filtration to afford the crude 5-phenylthiophene-2-carboxylic acid (178 mg). Step 2: A mixture of compound 5-phenylthiophene-2-carboxylic acid (118.5 mg, 0.58 mmol) in anhydrous DMF (2 mL)

were added EDC·HCl (188 mg, 2.0 mmol) and HOBt (112 mg, 1.6 mmol) at 0 ℃, and then compound **12b** (100 mg, 0.29 mmol) was added to the mixture after stirring for 15 min. The mixture was stirred at r.t for overnight, the reaction mixture was concentrated under reduced pressure. The residue was partitioned between CH_2Cl_2 and H_2O. The separated CH_2Cl_2 layer was washed with brine, dried over anhydrous Na_2SO_4 and evaporated to dryness, and then the residue was purified by column chromatography (eluting with CH_2Cl_2/MeOH by 100:1-20:1) to give compound **14f** (71 mg, 46% yield). ^{1}H NMR (500 MHz, DMSO-d_6) δ 9.57 (s, 1H), 9.39 (s, 1H), 8.08 (d, J = 2.9 Hz, 1H), 8.00 (d, J = 2.4 Hz, 1H), 7.75 (d, J = 7.5 Hz, 2H), 7.67 (s, 1H), 7.60 (d, J = 3.5 Hz, 1H), 7.53 (d, J = 8.5 Hz, 1H), 7.47 (t, J = 7.4 Hz, 2H), 7.39 (t, J = 7.3 Hz, 1H), 7.30 (d, J = 8.6 Hz, 1H), 4.53 (d, J = 12.8 Hz, 2H), 3.85 (s, 3H), 3.09 – 3.08 (m, 2H), 2.74 – 2.64 (m, 2H), 1.18 (d, J = 5.5 Hz, 6H). HPLC purity: 97.0%, R_t = 6.42 mim. HR MS (ESI): calcd for $C_{28}H_{30}FN_6O_2S$ $[M + H]^+$ 533.2129, found 533.2129.

5-(2-Chlorophenyl)-*N*-(4-((2-((3*S*,5*R*)-3,5-dimethyl-1-piperazinyl)-5-fluoro-4-pyrimidinyl)amino)-2-methoxyphenyl)thiophene-2-carboxamide (14g). Compound **14g** (72% yield) was obtained through the similar synthetic route of compound **14f**, except replacing phenylboronic acid with 2-chlorophenylboronic acid. ^{1}H NMR (500 MHz, DMSO-d_6) δ 9.66 (s, 1H), 9.48 (s, 1H), 8.11 (d, J = 3.5 Hz, 1H), 8.03 (d, J = 3.5 Hz, 1H), 7.71 (dd, J = 7.0, 2.3 Hz, 1H), 7.63 (dd, J = 6.9, 1.9 Hz, 2H), 7.52 (dd, J = 7.9, 6.4 Hz, 2H), 7.48 – 7.44 (m, 2H), 7.33 (dd, J = 8.6, 1.9 Hz, 1H), 4.61 (d, J = 13.0 Hz, 2H), 3.85 (s, 3H), 3.30 – 3.29 (m, 2H), 2.91 – 2.89 (m, 2H), 1.29 (d, J = 6.3 Hz, 6H). HPLC purity: 97.7%, R_t = 6.87 mim. HR MS (ESI): calcd for

$C_{28}H_{29}ClFN_6O_2S$ $[M + H]^+$ 567.1740, found 567.1752.

***N*-(4-((2-((3*S*,5*R*)-3,5-Dimethyl-1-piperazinyl)-5-fluoro-4-pyrimidinyl)amino)-2-methoxyphenyl)-5-(2-methoxyphenyl)thiophene-2-carboxamide (14h)**. Compound **14h** (76% yield) was obtained through the similar synthetic route of compound **14f**, except replacing phenylboronic acid with 2-methoxyphenylboronic acid. ^{1}H NMR (500 MHz, DMSO-d_6) δ 9.49 (s, 1H), 9.45 (s, 1H), 8.10 (s, 1H), 7.96 (s, 1H), 7.83 (d, J = 5.6 Hz, 1H), 7.67 (s, 1H), 7.62 (s, 1H), 7.56 (d, J = 7.3 Hz, 1H), 7.38 (s, 1H), 7.32 (d, J = 6.2 Hz, 1H), 7.19 (d, J = 6.8 Hz, 1H), 7.07 (d, J = 5.5 Hz, 1H), 4.61 (d, J = 11.4 Hz, 2H), 3.95 (s, 3H), 3.85 (s, 3H), 3.29 – 3.19 (m, 2H), 2.96 – 2.81 (m, 2H), 1.29 (d, J = 1.2 Hz, 6H). HPLC purity: 98.2%, R_t = 6.44 mim. HR MS (ESI): calcd for $C_{29}H_{32}FN_6O_3S$ $[M + H]^+$ 563.2235, found 563.2236.

***N*-(4-((2-((3*S*,5*R*)-3,5-Dimethyl-1-piperazinyl)-5-fluoro-4-pyrimidinyl)amino)-2-methoxyphenyl)-5-(o-tolyl)thiophene-2-carboxamide (14i)**. Compound **14i** (65% yield) was obtained through the similar synthetic route of compound **14f**, except replacing phenylboronic acid with 2-methylphenylboronic acid. ^{1}H NMR (500 MHz, DMSO-d_6) δ 9.57 (s, 1H), 9.29 (s, 1H), 8.03 (d, J = 3.6 Hz, 1H), 8.00 (d, J = 3.6 Hz, 1H), 7.76 (d, J = 2.1 Hz, 1H), 7.49 (d, J = 8.6 Hz, 1H), 7.46 – 7.44 (m, 1H), 7.38 – 7.25 (m, 5H), 4.40 (d, J = 10.2 Hz, 2H), 3.85 (s, 3H), 2.74 – 2.67 (m, 2H), 2.43 (s, 3H), 2.35 – 2.29 (m, 2H), 1.00 (d, J = 6.2 Hz, 6H). HPLC purity: 97.4%, R_t = 6.99 mim. HR MS (ESI): calcd for $C_{29}H_{32}FN_6O_2S$ $[M + H]^+$ 547.2286, found 547.2293.

5-(1-Cyclopentenyl)-*N*-(4-((2-((3*S*,5*R*)-3,5-dimethyl-1-piperazinyl)-5-fluoro-4-pyrimidinyl)amino)-2-methoxyphenyl)thiophene-2-carboxamide (14j). Compound

14j (70% yield) was obtained through the similar synthetic route of compound **14f**, except replacing phenylboronic acid with cyclopentenyl-1-boronic acid. ^{1}H NMR (500 MHz, DMSO-d_6) δ 9.47 (s, 1H), 9.36 (s, 1H), 8.07 (d, J = 3.5 Hz, 1H), 7.89 (d, J = 3.7 Hz, 1H), 7.67 (s, 1H), 7.52 (d, J = 8.6 Hz, 1H), 7.29 (d, J = 8.6 Hz, 1H), 7.11 (d, J = 3.8 Hz, 1H), 6.24 (s, 1H), 4.51 (d, J = 12.6 Hz, 2H), 3.84 (s, 3H), 3.18 (d, J = 1.7 Hz, 1H), 3.04 – 3.01 (m, 2H), 2.70 – 2.66 (m, 2H), 2.62 – 2.57 (m, 2H), 2.02 – 1.96 (m, 2H), 1.24 (s, 2H), 1.14 (d, J = 5.9 Hz, 6H). HPLC purity: 98.8%, R_t = 7.00 mim. HR MS (ESI): calcd for $C_{27}H_{32}FN_6O_2S$ $[M + H]^+$ 523.2286, found 523.2290.

5-(1-Cyclohexenyl)-*N*-(4-((2-((3*S*,5*R*)-3,5-dimethyl-1-piperazinyl)-5-fluoro-4-pyrimidinyl)amino)-2-methoxyphenyl)thiophene-2-carboxamide (14k). Compound **14k** (78% yield) was obtained through the similar synthetic route of compound **14f**, except replacing phenylboronic acid with cyclohexenyl-1-boronic acid. ^{1}H NMR (500 MHz, DMSO-d_6) δ 9.43 – 9.42 (m, 2H), 8.10 (d, J = 3.6 Hz, 1H), 7.86 (d, J = 3.9 Hz, 1H), 7.60 (d, J = 1.9 Hz, 1H), 7.53 (d, J = 8.6 Hz, 1H), 7.31 (dd, J = 8.7, 2.1 Hz, 1H), 7.12 (d, J = 3.9 Hz, 1H), 6.32 (s, 1H), 4.60 (d, J = 13.0 Hz, 2H), 3.84 (s, 3H), 3.29 – 3.24 (m, 2H), 2.87 – 2.81 (m, 2H), 2.41 – 2.35 (m, 2H), 2.19 (d, J = 3.6 Hz, 2H), 1.72 (dd, J = 7.6, 4.1 Hz, 2H), 1.61 (dd, J = 7.5, 4.0 Hz, 2H), 1.25 (d, J = 6.2 Hz, 6H). HPLC purity: 97.3%, R_t = 7.63 mim. HR MS (ESI): calcd for $C_{28}H_{34}FN_6O_2S$ $[M + H]^+$ 537.2442, found 537.2447.

***N*-(4-((2-((3*S*,5*R*)-3,5-Dimethyl-1-piperazinyl)-5-fluoro-4-pyrimidinyl)amino)-2-methoxyphenyl)-5-(3-furanyl)thiophene-2-carboxamide (14l)**. Compound **14l** (76% yield) was synthesized according to the similar synthetic route of compound **14f**, except

replacing phenylboronic acid with 3-furanboronic acid. ^{1}H NMR (500 MHz, DMSO-d_6) δ 9.53 (s, 1H), 9.44 (s, 1H), 8.23 (s, 1H), 8.10 (d, J = 3.0 Hz, 1H), 7.95 (s, 1H), 7.80 (s, 1H), 7.62 (s, 1H), 7.54 (d, J = 8.5 Hz, 1H), 7.37 (d, J = 3.5 Hz, 1H), 7.32 (d, J = 8.6 Hz, 1H), 6.92 (s, 1H), 4.61 (d, J = 12.6 Hz, 2H), 3.85 (s, 3H), 3.31 – 3.24 (m, 2H), 2.90 – 2.89 (m, 2H), 1.28 (d, J = 5.4 Hz, 6H). HPLC purity: 98.1%, R_t = 5.12 mim. HR MS (ESI): calcd for $C_{26}H_{28}FN_6O_3S$ $[M + H]^+$ 523.1922, found 523.1927.

Cell Culture and Animals. Human DLBCL cells SUDHL4, Farage and TOLEDO were purchased from American Type Culture Collection (ATCC). DOHH2 and OCI-Ly7 were from the DSMZ German collection of microorganisms and cell cultures. Human prostatic cell PNT1A was obtained from the European Collection of Authenticated Cell Cultures (ECACC). Normal human colon mucosal epithelial cell line NCM460, normal human hepatic cell line LO2 and human fibroblast cell line HAF were also from American Type Culture Collection (ATCC). DLBCL cell lines SUDHL-4, Farage, DOHH2 and TOLEDO were cultured in RPMI-1640 Medium (Gibco, C11875500BT), and DLBCL cell line OCI-Ly7 was grown in Iscove's Modified Dulbecco's Medium (Gibco, C11995500BT). Normal cell lines LO2, NCM460 and PNT1A were cultured in RPMI-1640 and HAF was maintained in DMEM with 2 mM of glutamine. Medium was supplemented with 10% FBS (Gibco, 10099141) and 1% penicillin-streptomycin (Gibco, 15140122). All cells were maintained at 37 ℃ of 5% humidified CO_2.

C57BL/6 mice and SCID mice were obtained from the National Rodent Laboratory Animal Resources, Shanghai Branch of China. All animal experimental protocols were

approved by the animal investigation committee of the Institute of Biomedical Sciences, East China Normal University. Compounds **2** and **3** were synthesized by the methods described in the literature.[32, 35]

BCL6 Protein and SMRT Peptide. The protein BCL6 BTB domain (5-129)[27] with C8Q, C67R, and C84N was synthesized expressed with C-terminal GST tagin E. coli BL21 (DE3). Proteins were purified using glutathione Sepharose 4B (GE Healthcare) and eluted with 10 mM of glutathione in 50 mM of Tris-HCl (pH 8.0), dialyzed with PBS, and concentrated. The peptide SMRT (1414-1430) with 6His tag was synthesized by Abace Biology Company.[27] These materials were used in the HTRF assay and Biolayer interferometry assay.

Homogenous Time Resolved Fluorescence (HTRF) Assay. HTRF assay was conducted according to the manufacturer's protocol (Cisbio). A total of 20 μL of final volume per well was added in 384-well plate (Greiner Bio-one, 784045). First, 2 μL of diluent buffer (Cisbio, 62DL3DDD) (or compounds dissolved in dilutent buffer) was added to each well, and 4 μL of BCL6-GST protein and 4 μL of 6His-SMRT peptide were then added. Plate was incubated at room temperature, 5 μL of anti-6His-XL665 (Cisbio, 61HISXLB) and 5 μL of anti-GST-Tb (Cisbio, 61GSTTLB) were added after 1 h. The plate was incubated for overnight and read on microplate reader (BioTek Cytation5) at 665 nm and 620 nm.

Real-Time Quantitative PCR. DLBCL cells were exposed to compounds for 24 h**.** Total RNA was extracted with Trizol (Invitrogen) and reversely transcripted into cDNA with Prime Script RT Kit (Takara). We amplified specific genes with the following

primers:

P53: CCCTTCCCAGAAAACCTACC and AATCAACCCACAGCTGCAC,

ATR: AAGCGCCACTGAATGAAACT and GTCGCTGCTCAATGTCAAGA,

CXCR4: AGGCCCTAGCTTTCTTCCAC and CTGCTCACAGAGGTGAGTGC,

CDKN1A: CTGAAGGGTCCCCAGGTG and TAGGGCTTCCTCTTGGAGAA,

CD69: CTGGTCACCCATGGAAGTG and CATGCTGCTGACCTCTGTGT,

CD80: CATCCTGGGCCATTACCTTA and TCTCTCTCTGCATCTTGGGG,

β-actin: TGAAGTGTGACGTGGACATC and CATACTCCTGCTTGCTGATC. All reactions were repeated three times.

Lentiviral packing, BCL6 knockdown and overexpression. DNA coding the shRNA sequence against BCL6 was subcloned into lentiviral vector LentiLox 3.7 (pLL3.7). Fragments of BCL6 were subcloned into the lentiviral expression vector PCDH. HEK293T cells were co-transfected with pLL3.7-shBCL6 or PCDH-BCL6 and packaging plasmids. Medium was replaced 6 h after transfection and virus supernatant was collected at 48 h and 72 h after transfection. DLBCL cells were infected with virus supplemented with 8 μg/mL of polybrene for 48 h. Then, the medium was replaced with fresh RPMI 1640 supplemented with 2 μg/mL puromycin.

Biolayer interferometry. The binding affinities between compounds and BCL6 protein were determined using Biolayer interferometry (BLI) on a ForteBIO Octet (Menlo Park, CA, USA). Experiments were performed using 1× kinetics buffer (1× PBS and 0.02% Tween 20) as the diluent. The GST biosensors (Fortebio, 18-5096) were hydrated in 1× kinetics buffer for 10 minutes before the tests and then dipped into

1× kinetics buffer for 60 s to establish a stable baseline before loading BCL6-GST protein (50 ng/mL) onto the sensors 300-600 s. After loading, another baseline in 1× kinetics buffer was established for 60 s before coated sensors were dipped into wells containing compounds in serial dilutions concentrations. The 60 s association step was followed by a dissociation step for 60 s. To control for nonspecific binding of compounds to sensors in the absence of BCL6-GST protein, reference sensors were used in parallel for each concentration of compounds and subtracted from total response. Data analyses were performed with ForteBio Data Analysis 10 software.

Germinal center formation. 8 weeks old male C57BL/6 mice were intraperitoneally injected with 100 μg 4-hydroxy-3-nitrophenylacetyl (NP) (santa cruz, sc-396297)-coupled chicken gamma globulin (CGG) (Cedarlane, CLF802-1). Two days later, mice were treated with 50 mg/kg/d of compound **2** by intraperitoneal injection and 10 mg/kg/3d of compound **14j** by tail intravenous injection. After 12 days of treatments, mice were euthanized and spleens and serum were collected.

Flow cytometric analysis. Single-cell suspensions were prepared and red blood cells were lysed by ACK. Antibodies used for staining were: PerCP/cy5.5-anti-B220 (Biolegend, 103236), FITC-anti-FAS (BD Pharmingen, 554257), eFluor660-anti-GL7 (Invitrogen, 50-5902-82), PerCP/cy5.5-anti-CD4 (Biolegend, 100434), PE-anti-CXCR5 (Biolegend, 145504), APC-anti-PD1(Biolegend, 109112). The stained cells were analyzed FACS Calibur (BD).

ELISA. T cell-dependent antibody production was detected by ELISA using the two coupling ratios of NP-BSA (NP23-BSA or NP5-BSA) as the coating Ags. Mouse

serum was collected and titers of anti-NP Abs were measured, according to the manufacturer's protocol (Southern Biotech). OD values determined at 450 nm.

Immunofluorescent staining. Spleens from mice were embedded in OCT (Sakura) and snap-frozen in liquid nitrogen bath. Frozen sections (6 μm in thickness) were fixed in ice-cold acetone for 15 minutes and air-dried. After rehydration in PBS, frozen sections were blocked in 10% BSA and stained with a mixture of biotin-conjugated peanut agglutinin (Sigma, L6135) and IgD (BD Pharmingen, 553438) at 4 ℃ for overnight. The sections were washed with PBS and subsequently stained with a mixture of donkey anti-rat IgG(H+L)-Alexa Fluor 488 (Invitrogen, A21208) and streptavidin-Cy3 (Biolegend, 405215) for 2 h at room temperature. Images were acquired by a fluorescence confocal microscope. The size and number of GCs were analyzed using image analysis software.

Cell Proliferation Assay. Cell viability was assessed by CCK8 kit (7sea biotech, C008-2) and EdU proliferation kit (Beyotime, C0071S). For CCK8 assay, cells (90 μL) were seeded in 96-well plate (2×10^4 cells/well), then treated with 10 × various concentrations of compound (10 μL). After 72 h, adding 10 μL of CCK8 to each well of the plates and incubated at 37 ℃ for 1-2 h. The absorption at 450 nm was measured by a microplate spectrophotometer. For EdU proliferation assay, cells were incubated with 10 μM of EdU solution for 2 h then fixed and permeabilized. Cells were stained with EdU/Alexa Fluor Azide 488 for 30 minutes and analyzed by flow cytometry. Experiments were performed in triplicate.

Cell apoptosis assay. DLBCL cells were cultured in 6-well plate with different

concentrations of compounds for 48 h. Cells were collected and washed with PBS, then resuspended in binding buffer and incubated with Annexin V-FITC and propidium iodide. About 15 minutes later, cells were analyzed immediately with flow cytometry (FACS Calibur, BD Biosciences).

Xenograft Model of DLBCL. SUDHL4 cells (1×10^7 cells/mouse) were subcutaneously injected into 6 weeks old male SCID mice. After the tumors reached about 100 mm^3, the mice were randomly divided into the indicated groups and the mice were treated by tail intravenous injection with 5 or 10 mg/kg/3d of **14j** or vehicle for 15 days. During the administration of drugs, the body weight and the tumor size of the mice were monitored every 3 days. Tumor volume was assessed by caliper measurement using the formula: tumor volume = length × width × width × 0.52.

Haematoxylin and eosin (H&E) and Immunohistochemistry (IHC). Tumors or tissue specimens were removed from sacrificing mice, fixed in 4% paraformaldehyde for 24 h, progressively dehydrated and embedded in paraffin. Sections were prepared and IHC was performed using anti–Ki67 (1:250; Catalog #ab15580, Abcam). H&E staining was carried out according to standard protocol with haematoxylin and eosin to indicate nucleus and cytoplasm, respectively.

Quantum Chemical Calculations. Initial structures of the new synthesized molecules were modeled with the aid of GaussView 6.0 and used as input geometry for charge distribution calculation. Molecules geometry optimizations and frequency calculations were carried out at B3LYP/6-31++G(d,p) level of theory with the Gaussian 16 software.[45] And the compounds optimized molecular structures were visualized

using GaussView 6.0.

Molecule Docking. Molecular docking studies between the new synthesized compounds (**13a**, **13c**, **14a**, **14f**, **14j** and **14l**) and $BCL6^{BTB}$ domain were performed using Autodock4.2.6.[46] The X-ray crystal structures of $BCL6^{BTB}$ domain co-crystallized with ligand pyrazolo-pyrimidine macrocyclic (PDB ID code: 5N1Z)[36] was downloaded from the protein data bank. The co-crystalized ligand was used to define the active sites for docking. A grid of 60, 60, and 60 points in x, y and z direction was created with a grid spacing of 0.375 Å at the binding site for the docking between target compounds and $BCL6^{BTB}$ domain, respectively. The program AutoDockTool 1.5.6 was used for preparing the parameter files between target compounds and $BCL6^{BTB}$ domain. Protonation states for titratable residues of BCL6 (including His14) were assigned using H++,[47] which accounts for each of the 2^N protonation microstates (when N titratable residues are active). In our calculation, His14 of BCL6 prefers a neutral protonation state (HIE, with the single proton on Nε) at pH = 7.4, which is consistent with our experimental pH value. The Lamarckian genetic algorithm was used to generate the binding poses between target compounds and $BCL6^{BTB}$ domain.[48] 200 docking runs for every target compounds bound to $BCL6^{BTB}$ domain were calculated with the rotation of all non-ring torsion angles. The docking conformations with the lowest binding energy were selected for analysis, respectively.

Statistical analysis. We expressed data as mean ± SD. Significance between groups was determined by Student's test using GraphPad Prism 5.0. For animal experiments, we used two-way ANOVA. All experiments were performed at least three times except

for animal experiments. The significant differences were considered at the level of *P < 0.05, ** P < 0.01 and ***P < 0.001.

Supporting Information

The Supporting Information is available free of charge on the ACS Publications website. The optimized structures with charge distribution of new synthesized $BCL6^{BTB}$ domain inhibitors (**13a**, **13c**, **14a**, **14f**, **14j** and **14l**)； shRNA-mediated knockdown of BCL6; Additional figures related biological studies; HPLC spectra of key target compounds (PDF)

Molecular formula strings (CSV)

AUTHOR INFORMATION

Corresponding Authors

*Y.C.: Phone: +86-21-24206647. Fax: +86-21-54344922. E-mail: yhchen@bio.ecnu.edu.cn

*Z.Y.: Phone: +86-21-54345016. Fax: +86-21-54344922. E-mail: zfyi@bio.ecnu.edu.cn

*M.L.: Phone: +86-21-54345014. Fax: +86-21-54344922. E-mail: myliu@bio.ecnu.edu.cn

Author Contributions

# W.G., and Y. X. contributed equally to this work.

Notes

The authors declare no competing financial interest.

ACKNOWLEDGMENTS

This work was supported by the grants from National Key R&D Program of China (2018YFA0507001, 2015CB910400), National Natural Science Foundation of China (81673304, 81973160, 81830083 and 81773204), Innovation program of Shanghai

municipal education commission (2017-01-07-00-05-E00011), Shenzhen Municipal Government of China (KQTD20170810160226082). ECNU Multifunctional Platform for Innovation (001 and 011).

ABBREVIATIONS USED

BCL6, B-Cell Lymphoma 6; GC, germinal center; Tfh, follicular helper T; DLBCL, diffuse large B cell lymphoma; TKIs, tyrosine kinase inhibitors; CML, chronic myeloid leukemia cells; ALL, acute lymphoblastic leukemia; BTB, Broad-Complex, tramtrack and Bric-a-brac; SMRT, silencing mediator for retinoid or thyroid hormone receptors; N-CoR, nuclear receptor Corepressor; BCoR, BCL6 corepressor; LG, lateral groove; DIEA, *N,N*-Diisopropylethylamine; DMF, dimethylformamide; HTRF, Homogeneous Time-Resolved Fluorescence;

Figure legends

Figure 1. Several known small molecular BCL6 inhibitors.

Figure 2. Design strategy and optimization direction based on initial hit compound. (A) Initial hit compound. (B) Design and synthesis of novel BCL6 inhibitors.

Figure 3. Binding poses obtained for compounds **13a** (blue, panel A), **13c** (yellow, panel B), **14a** (magenta, panel C), **14f** (wheat, panel D), **14j** (hotpink, panel E) and **14l** (lightpink, panel F) in BCL6 BTB domain (PDB code:5N1Z). The BCL6 BTB domain was shown as cyan cartoon, and the inter residues were shown as green sticks.

Figure 4. Compound **14j** specifically induces de-repression of BCL6 target genes. (A) SUDHL4 and Farage (both BCL6 dependent) DLBCL cell lines were exposed to compounds **2** (50 μM), **3** (5 μM) and **14j** (5 μM) for 24 h to measure mRNA expression

of the BCL6 target genes (p53, ATR, CXCR4, CD69 and CDKN1A) with RT-PCR. (B) mRNA abundance of p53, ATR, CDKN1A, CXCR4, CD69 and CD80 were measured in SUDLH4, Farage (both BCL6 dependent) and Toledo (BCL6 independent) DLBCL cell lines after treatments of **14j** with the doses of 1.25, 2.50 and 5.00 μM for 24 h. (*, $P < 0.05$; **, $P < 0.01$; ***, $P < 0.001$ versus control).

Figure 5. The K_D values of compounds binding to BCL6 proteins in Biolayer interferometry assay. Kinetic binding sensorgrams of compounds **2**, **3** and **14j** and the steady state fitting of the equilibrium responses *vs* compound concentrations based on 1:1 binding model.

Figure 6. Compound **14j** inhibits DLBCL growth and induces apoptosis *in vitro*. (A) The significant inhibitory effects of **14j** against SUDHL4 cells growth in the EdU Flow Cytometry assay. (B) The apoptosis effects of SUDHL4 cells after treatments with compounds **2**, **3** and **14j** for 48 h.

Figure 7. Compound **14j** impairs GC formation *in vivo*. C57BL/6 mice were immunized with NP-CGG and two days later by tail intravenous injection with the dose of **14j** at 10 mg/kg/3d for 12 days. (A) Flow cytometry detection of splenic GC B cells ($B220^+GL7^+FAS^+$) (left) and quantification (right). (*, $P < 0.05$; **, $P < 0.01$; ***, $P < 0.001$ versus control). (B) Splenic tissue was stained for peanut agglutinin (red) and IgD (green), scale bars represent 100 μm. (*, $P < 0.05$; **, $P < 0.01$; ***, $P < 0.001$ versus control). (C) Flow cytometry of Tfh cells ($CD4^+CXCR5^+PD1^+$) (left) and quantification (right). (*, $P < 0.05$; **, $P < 0.01$; ***, $P < 0.001$ versus control). (D) Titers of NP-specific immunoglobulin G1 antibody measured by ELISA with NP5-

BSA and NP23-BSA in serum from mice immunized with NP-CGG and presented in relative units (RU) as serial dilution of serum relative to antibody end-point titers. (*, $P < 0.05$; **, $P < 0.01$; ***, $P < 0.001$ versus control).

Figure 8. The anti-cancer effects of compound **14j** on DLBCL mouse xenograft model. (A) SUDHL4 cells were injected subcutaneously into 8-week-old male SCID mice. When vehicle controls reached maximal permitted tumor burden, tumors were removed and photographed. (B) Tumor volumes were measured every 3 days. (*, $P < 0.05$; **, $P < 0.01$; ***, $P < 0.001$ versus control). (C) The weights of removed tumors. (*, $P < 0.05$; **, $P < 0.01$; ***, $P < 0.001$ versus control). (D) Change of mice body weights with the treatments of different compounds. (E) IHC of tumors stained with Ki67. Scale bars, 50 μm. (***, $P < 0.001$ versus control). (F) qPCR was performed in pulverized tumors from the mice to measure the mRNA expression of the BCL6 target genes CD69, CXCR4 and ATR. (*, $P < 0.05$; **, $P < 0.01$; ***, $P < 0.001$ versus control).

REFERENCES

1. Tahara, K.; Takizawa, M.; Yamane, A.; Osaki, Y.; Ishizaki, T.; Mitsui, T.; Yokohama, A.; Saitoh, T.; Tsukamoto, N.; Matsumoto, M.; Murakami, H.; Nojima, Y.; Handa, H. Overexpression of B-cell lymphoma 6 alters gene expression profile in a myeloma cell line and is associated with decreased DNA damage response. *Cancer Sci.* **2017,** 108, 1556-1564.

2. Ye, B. H.; Lista, F.; Lo Coco, F.; Knowles, D. M.; Offit, K.; Chaganti, R. S.; Dalla-Favera, R. Alterations of a zinc finger-encoding gene, BCL6, in diffuse large-cell lymphoma. *Science* **1993,** 262, 747-750.

3. Baron, B. W.; Nucifora, G.; McCabe, N.; Espinosa, R., 3rd; Le Beau, M. M.; McKeithan, T. W. Identification of the gene associated with the recurring chromosomal translocations t(3;14)(q27;q32) and t(3;22)(q27;q11) in B-cell lymphomas. *Proc. Natl. Acad. Sci. USA.* **1993,** 90, 5262-5266.

4. Basso, K.; Dalla-Favera, R. Roles of BCL6 in normal and transformed germinal center B cells. *Immunol. Rev.* **2012,** 247, 172-183.

5. Basso, K.; Dalla-Favera, R. BCL6: master regulator of the germinal center reaction and key oncogene in B cell lymphomagenesis. *Adv. Immunol.* **2010,** 105, 193-210.

6. Polo, J. M.; Juszczynski, P.; Monti, S.; Cerchietti, L.; Ye, K.; Greally, J. M.; Shipp, M.; Melnick, A. Transcriptional signature with differential expression of BCL6 target genes accurately identifies BCL6-dependent diffuse large B cell lymphomas. *Proc. Natl. Acad. Sci. USA.* **2007,** 104, 3207-3212.

7. Ci, W.; Polo, J. M.; Cerchietti, L.; Shaknovich, R.; Wang, L.; Yang, S. N.; Ye, K.; Farinha, P.; Horsman, D. E.; Gascoyne, R. D.; Elemento, O.; Melnick, A. The BCL6 transcriptional program features repression of multiple oncogenes in primary B cells and is deregulated in DLBCL. *Blood* **2009,** 113, 5536-5548.

8. Parekh, S.; Prive, G.; Melnick, A. Therapeutic targeting of the BCL6 oncogene for diffuse large B-cell lymphomas. *Leuk. Lymphoma* **2008,** 49, 874-882.

9. Ranuncolo, S. M.; Polo, J. M.; Dierov, J.; Singer, M.; Kuo, T.; Greally, J.; Green, R.; Carroll, M.; Melnick, A. BCL6 mediates the germinal center B cell phenotype and lymphomagenesis through transcriptional repression of the DNA-damage sensor ATR. *Nat. Immunol.* **2007,** 8, 705-714.

10. Cerchietti, L. C.; Polo, J. M.; Da Silva, G. F.; Farinha, P.; Shaknovich, R.; Gascoyne, R. D.; Dowdy, S. F.; Melnick, A. Sequential transcription factor targeting for diffuse large B-cell lymphomas. *Cancer Res.* **2008,** 68, 3361-3369.

11. Cerchietti, L. C.; Yang, S. N.; Shaknovich, R.; Hatzi, K.; Polo, J. M.; Chadburn, A.; Dowdy, S. F.; Melnick, A. A peptomimetic inhibitor of BCL6 with potent antilymphoma effects in vitro and in vivo. *Blood* **2009,** 113, 3397-3405.

12. Logarajah, S.; Hunter, P.; Kraman, M.; Steele, D.; Lakhani, S.; Bobrow, L.; Venkitaraman, A.; Wagner, S. BCL6 is expressed in breast cancer and prevents mammary epithelial differentiation. *Oncogene* **2003,** 22, 5572-5578.

13. Bos, R.; van Diest, P. J.; van der Groep, P.; Greijer, A. E.; Hermsen, M. A.; Heijnen, I.; Meijer, G. A.; Baak, J. P.; Pinedo, H. M.; van der Wall, E.; Shvarts, A. Protein expression of B-cell lymphoma gene 6 (BCL6) in invasive breast cancer is associated with cyclin D1 and hypoxia-inducible factor-1alpha (HIF-1alpha). *Oncogene* **2003,** 22, 8948-8951.

14. Walker, S. R.; Liu, S.; Xiang, M.; Nicolais, M.; Hatzi, K.; Giannopoulou, E.; Elemento, O.; Cerchietti, L.; Melnick, A.; Frank, D. A. The transcriptional modulator BCL6 as a molecular target for breast cancer therapy. *Oncogene* **2015,** 34, 1073-1082.

15. Xu, L.; Chen, Y.; Dutra-Clarke, M.; Mayakonda, A.; Hazawa, M.; Savinoff, S. E.; Doan, N.; Said, J. W.; Yong, W. H.; Watkins, A.; Yang, H.; Ding, L. W.; Jiang, Y. Y.; Tyner, J. W.; Ching, J.; Kovalik, J. P.; Madan, V.; Chan, S. L.; Muschen, M.; Breunig, J. J.; Lin, D. C.; Koeffler, H. P. BCL6 promotes glioma and serves as a therapeutic target. *Proc. Natl. Acad. Sci. USA.* **2017,** 114, 3981-3986.

16. Ruggieri, S.; Tamma, R.; Marzullo, A.; Annese, T.; Marinaccio, C.; Errede, M.; Susca, F. C.; Senetta, R.; Cassoni, P.; Vacca, A.; Albano, F.; Saracino, C.; Notarangelo, A.; Specchia, G.; Ribatti, D.; Nico, B. Translocation of the proto-oncogene BCL6 in human glioblastoma multiforme. *Cancer Lett.* **2014,** 353, 41-51.

17. Zhu, L.; Feng, H.; Jin, S.; Tan, M.; Gao, S.; Zhuang, H.; Hu, Z.; Wang, H.; Song, Z.; Lin, B. High expressions of BCL6 and Lewis y antigen are correlated with high tumor burden and poor prognosis in epithelial ovarian cancer. *Tumour Biol.* **2017,** 39, 1-12.

18. Deb, D.; Rajaram, S.; Larsen, J. E.; Dospoy, P. D.; Marullo, R.; Li, L. S.; Avila, K.; Xue, F. T.; Cerchietti, L.; Minna, J. D.; Altschuler, S. J.; Wu, L. F. Combination therapy targeting BCL6 and phospho-STAT3 defeats intratumor heterogeneity in a subset of non-small cell lung cancers. *Cancer Res.* **2017,** 77, 3070-3081.

19. Madapura, H. S.; Nagy, N.; Ujvari, D.; Kallas, T.; Krohnke, M. C. L.; Amu, S.; Bjorkholm, M.; Stenke, L.; Mandal, P. K.; McMurray, J. S.; Keszei, M.; Westerberg, L. S.; Cheng, H.; Xue, F.; Klein, G.; Klein, E.; Salamon, D. Interferon gamma is a STAT1-dependent direct inducer of BCL6 expression in imatinib-treated chronic myeloid leukemia cells. *Oncogene* **2017,** 36, 4619-4628.

20. Hurtz, C.; Hatzi, K.; Cerchietti, L.; Braig, M.; Park, E.; Kim, Y. M.; Herzog, S.; Ramezani-Rad, P.; Jumaa, H.; Muller, M. C.; Hofmann, W. K.; Hochhaus, A.; Ye, B. H.; Agarwal, A.; Druker, B. J.; Shah, N. P.; Melnick, A. M.; Muschen, M. BCL6-mediated repression of p53 is critical for leukemia stem cell survival in chronic myeloid leukemia. *J. Exp. Med.* **2011,** 208, 2163-2174.

21. Duy, C.; Hurtz, C.; Shojaee, S.; Cerchietti, L.; Geng, H.; Swaminathan, S.; Klemm, L.; Kweon, S. M.; Nahar, R.; Braig, M.; Park, E.; Kim, Y. M.; Hofmann, W. K.; Herzog, S.; Jumaa, H.; Koeffler, H. P.; Yu, J. J.; Heisterkamp, N.; Graeber, T. G.; Wu, H.; Ye, B. H.; Melnick, A.; Muschen, M. BCL6 enables Ph+ acute lymphoblastic leukaemia cells to survive BCR-ABL1 kinase inhibition. *Nature* **2011,** 473, 384-388.

22. Dupont, T.; Yang, S. N.; Patel, J.; Hatzi, K.; Malik, A.; Tam, W.; Martin, P.; Leonard, J.; Melnick, A.; Cerchietti, L. Selective targeting of BCL6 induces oncogene addiction switching to BCL2 in B-cell lymphoma. *Oncotarget* **2016,** 7, 3520-3532.

23. Cattoretti, G.; Chang, C. C.; Cechova, K.; Zhang, J.; Ye, B. H.; Falini, B.; Louie, D. C.; Offit, K.; Chaganti, R. S.; Dalla-Favera, R. BCL6 protein is expressed in germinal-center B cells. *Blood* **1995,** 86, 45-53.

24. Onizuka, T.; Moriyama, M.; Yamochi, T.; Kuroda, T.; Kazama, A.; Kanazawa, N.; Sato, K.; Kato, T.; Ota, H.; Mori, S. BCL6 gene product, a 92- to 98-kD nuclear phosphoprotein, is highly expressed in germinal center B cells and their neoplastic counterparts. *Blood* **1995,** 86, 28-37.

25. Huynh, K. D.; Bardwell, V. J. The BCL6 POZ domain and other POZ domains interact with the co-repressors N-CoR and SMRT. *Oncogene* **1998,** 17, 2473-2484.

26. Dhordain, P.; Albagli, O.; Lin, R. J.; Ansieau, S.; Quief, S.; Leutz, A.; Kerckaert, J. P.; Evans, R. M.; Leprince, D. Corepressor SMRT binds the BTB/POZ repressing domain of the LAZ3/BCL6 oncoprotein. *Proc. Natl. Acad. Sci. USA.* **1997,** 94, 10762-10767.

27. Ahmad, K. F.; Melnick, A.; Lax, S.; Bouchard, D.; Liu, J.; Kiang, C. L.; Mayer, S.;

Takahashi, S.; Licht, J. D.; Prive, G. G. Mechanism of SMRT corepressor recruitment by the BCL6 BTB domain. *Mol. Cell* **2003,** 12, 1551-1564.

28. Huynh, K. D.; Fischle, W.; Verdin, E.; Bardwell, V. J. BCoR, a novel corepressor involved in BCL-6 repression. *Genes Dev.* **2000,** 14, 1810-1823.

29. Polo, J. M.; Dell'Oso, T.; Ranuncolo, S. M.; Cerchietti, L.; Beck, D.; Da Silva, G. F.; Prive, G. G.; Licht, J. D.; Melnick, A. Specific peptide interference reveals BCL6 transcriptional and oncogenic mechanisms in B-cell lymphoma cells. *Nat. Med.* **2004,** 10, 1329-1335.

30. Huang, C.; Hatzi, K.; Melnick, A. Lineage-specific functions of BCL6 in immunity and inflammation are mediated by distinct biochemical mechanisms. *Nat. Immunol.* **2013,** 14, 380-388.

31. Cerchietti, L. C.; Ghetu, A. F.; Zhu, X.; Da Silva, G. F.; Zhong, S.; Matthews, M.; Bunting, K. L.; Polo, J. M.; Fares, C.; Arrowsmith, C. H.; Yang, S. N.; Garcia, M.; Coop, A.; Mackerell, A. D., Jr.; Prive, G. G.; Melnick, A. A small-molecule inhibitor of BCL6 kills DLBCL cells in vitro and in vivo. *Cancer Cell* **2010,** 17, 400-411.

32. Cardenas, M. G.; Yu, W.; Beguelin, W.; Teater, M. R.; Geng, H.; Goldstein, R. L.; Oswald, E.; Hatzi, K.; Yang, S. N.; Cohen, J.; Shaknovich, R.; Vanommeslaeghe, K.; Cheng, H.; Liang, D.; Cho, H. J.; Abbott, J.; Tam, W.; Du, W.; Leonard, J. P.; Elemento, O.; Cerchietti, L.; Cierpicki, T.; Xue, F.; MacKerell, A. D., Jr.; Melnick, A. M. Rationally designed BCL6 inhibitors target activated B cell diffuse large B cell lymphoma. *J. Clin. Invest.* **2016,** 126, 3351-3362.

33. Cheng, H.; Linhares, B. M.; Yu, W.; Cardenas, M. G.; Ai, Y.; Jiang, W.; Winkler,

A.; Cohen, S.; Melnick, A.; MacKerell, A., Jr.; Cierpicki, T.; Xue, F. Identification of thiourea-based inhibitors of the B-cell lymphoma 6 BTB domain via NMR-based fragment screening and computer-aided drug design. *J. Med. Chem.* **2018,** 61, 7573-7588.

34. Mendgen, T.; Steuer, C.; Klein, C. D. Privileged scaffolds or promiscuous binders: a comparative study on rhodanines and related heterocycles in medicinal chemistry. *J. Med. Chem.* **2012,** 55, 743-753.

35. Kamada, Y.; Sakai, N.; Sogabe, S.; Ida, K.; Oki, H.; Sakamoto, K.; Lane, W.; Snell, G.; Iida, M.; Imaeda, Y.; Sakamoto, J.; Matsui, J. Discovery of a B-cell lymphoma 6 protein-protein interaction inhibitor by a biophysics-driven fragment-based approach. *J. Med. Chem.* **2017,** 60, 4358-4368.

36. McCoull, W.; Abrams, R. D.; Anderson, E.; Blades, K.; Barton, P.; Box, M.; Burgess, J.; Byth, K.; Cao, Q.; Chuaqui, C.; Carbajo, R. J.; Cheung, T.; Code, E.; Ferguson, A. D.; Fillery, S.; Fuller, N. O.; Gangl, E.; Gao, N.; Grist, M.; Hargreaves, D.; Howard, M. R.; Hu, J.; Kemmitt, P. D.; Nelson, J. E.; O'Connell, N.; Prince, D. B.; Raubo, P.; Rawlins, P. B.; Robb, G. R.; Shi, J.; Waring, M. J.; Whittaker, D.; Wylot, M.; Zhu, X. Discovery of pyrazolo[1,5-a]pyrimidine B-cell lymphoma 6 (BCL6) binders and optimization to high affinity macrocyclic inhibitors. *J. Med. Chem.* **2017,** 60, 4386-4402.

37. Kerres, N.; Steurer, S.; Schlager, S.; Bader, G.; Berger, H.; Caligiuri, M.; Dank, C.; Engen, J. R.; Ettmayer, P.; Fischerauer, B.; Flotzinger, G.; Gerlach, D.; Gerstberger, T.; Gmaschitz, T.; Greb, P.; Han, B.; Heyes, E.; Iacob, R. E.; Kessler, D.; Kolle, H.;

Lamarre, L.; Lancia, D. R.; Lucas, S.; Mayer, M.; Mayr, K.; Mischerikow, N.; Muck, K.; Peinsipp, C.; Petermann, O.; Reiser, U.; Rudolph, D.; Rumpel, K.; Salomon, C.; Scharn, D.; Schnitzer, R.; Schrenk, A.; Schweifer, N.; Thompson, D.; Traxler, E.; Varecka, R.; Voss, T.; Weiss-Puxbaum, A.; Winkler, S.; Zheng, X.; Zoephel, A.; Kraut, N.; McConnell, D.; Pearson, M.; Koegl, M. Chemically induced degradation of the oncogenic transcription factor BCL6. *Cell Rep.* **2017,** 20, 2860-2875.

38. Zhou, W.; Huang, A.; Zhang, Y.; Lin, Q.; Guo, W.; You, Z.; Yi, Z.; Liu, M.; Chen, Y. Design and optimization of hybrid of 2,4-diaminopyrimidine and arylthiazole scaffold as anticancer cell proliferation and migration agents. *Eur. J. Med. Chem.* **2015,** 96, 269-280.

39. Hatzi, K.; Melnick, A. Breaking bad in the germinal center: how deregulation of BCL6 contributes to lymphomagenesis. *Trends Mol. Med.* **2014,** 20, 343-352.

40. Zhou, H.; Lu, J.; Liu, L.; Bernard, D.; Yang, C. Y.; Fernandez-Salas, E.; Chinnaswamy, K.; Layton, S.; Stuckey, J.; Yu, Q.; Zhou, W.; Pan, Z.; Sun, Y.; Wang, S. A potent small-molecule inhibitor of the DCN1-UBC12 interaction that selectively blocks cullin 3 neddylation. *Nat. Commun.* **2017,** 8, No, 1150.

41. Hammitzsch, A.; Tallant, C.; Fedorov, O.; O'Mahony, A.; Brennan, P. E.; Hay, D. A.; Martinez, F. O.; Al-Mossawi, M. H.; de Wit, J.; Vecellio, M.; Wells, C.; Wordsworth, P.; Muller, S.; Knapp, S.; Bowness, P. CBP30, a selective CBP/p300 bromodomain inhibitor, suppresses human Th17 responses. *Proc. Natl. Acad. Sci. USA.* **2015,** 112, 10768-10773.

42. Cardenas, M. G.; Oswald, E.; Yu, W.; Xue, F.; MacKerell, A. D., Jr.; Melnick, A.

M. The expanding role of the BCL6 oncoprotein as a cancer therapeutic target. *Clin. Cancer Res.* **2017,** 23, 885-893.

43. Klein, U.; Dalla-Favera, R. Germinal centres: role in B-cell physiology and malignancy. *Nat. Rev. Immunol.* **2008,** 8, 22-33.

44. Nurieva, R. I.; Chung, Y.; Martinez, G. J.; Yang, X. O.; Tanaka, S.; Matskevitch, T. D.; Wang, Y. H.; Dong, C. BCL6 mediates the development of T follicular helper cells. *Science* **2009,** 325, 1001-1005.

45. Frisch, M.; Trucks, G.; Schlegel, H.; Scuseria, G.; Robb, M.; Cheeseman, J.; Scalmani, G.; Barone, V.; Petersson, G.; Nakatsuji, H. Gaussian 16. *Revision A* **2016,** 3.

46. Morris, G. M.; Huey, R.; Lindstrom, W.; Sanner, M. F.; Belew, R. K.; Goodsell, D. S.; Olson, A. J. AutoDock4 and AutoDockTools4: Automated docking with selective receptor flexibility. *J. Comput. Chem.* **2009,** 30, 2785-2791.

47. Anandakrishnan, R.; Aguilar, B.; Onufriev, A. V. H++ 3.0: automating pK prediction and the preparation of biomolecular structures for atomistic molecular modeling and simulations. *Nucleic Acids Res.* **2012,** 40, W537-541.

48. Morris, G. M.; Goodsell, D. S.; Halliday, R. S.; Huey, R.; Hart, W. E.; Belew, R. K.; Olson, A. J. Automated docking using a lamarckian genetic algorithm and an empirical binding free energy function. *J. Comput. Chem.* **1998,** 19, 1639-1662.

Table 1. HTRF Affinities between Compounds 9a-n and BCL6 BTB domain.

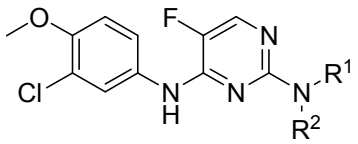

Compd.	NR^1R^2	BCL6 HTRF IC_{50} (μM)	Compd.	NR^1R^2	BCL6 HTRF IC_{50} (μM)
9a		4.96 ± 0.8	**9h**	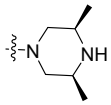	0.77 ± 0.05
9b		4.83 ± 0.4	**9i**	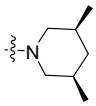	>10
9c	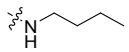	>10	**9j**	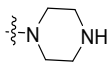	0.98 ± 0.01
9d	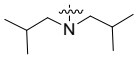	>10	**9k**	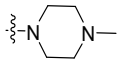	1.12 ± 0.3
9e	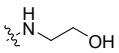	2.44 ± 0.3	**9l**		2.59 ± 0.4
9f	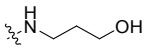	0.86 ± 0.01	**9m**	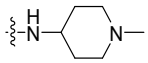	0.89 ± 0.08
9g	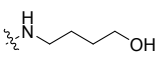	2.04 ± 0.1	**9n**	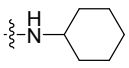	7.41 ± 4.0
2(FX1)	-	37.7 ± 3.6	**3**	-	0.45 ± 0.1

Table 2. HTRF Affinities between Compounds 13a-f and BCL6 BTB domain.

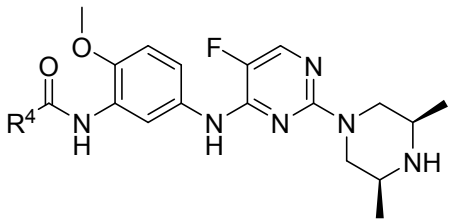

Compd.	R^4	BCL6 HTRF IC_{50} (μM)	Compd.	R^4	BCL6 HTRF IC_{50} (μM)
13a	5-Br-thiopheneyl	>20	**13e**	6-F-2-Py	14.9 ± 0.2
13b	5-Br-furanyl	>20	**13f**	6-Br-2-Py	17.3 ± 1.2
13c	3-Br-Ph	7.72 ± 0.2	**2**	-	37.7 ± 3.6
13d	2-Py	9.56 ± 2.4	**3**	-	0.45 ± 0.1

Table 3. HTRF Affinities between Compounds 14a-l and BCL6 BTB domain.

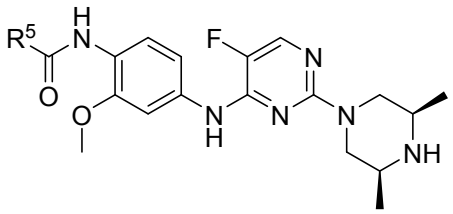

Compd.	R^5	BCL6 HTRF IC_{50} (μM)	Compd.	R^5	BCL6 HTRF IC_{50} (μM)
14a	3-Br-Ph	1.85 ± 0.3	**14h**	5-(2-MeO-Ph)thiopheneyl	2.46 ± 0.5
14b	5-Br-furanyl	>10	**14i**	5-(2-Me-Ph)thiopheneyl	1.73 ± 0.2
14c	6-Br-2-Py	3.44 ± 1.5	**14j**	5-(1-Cyclopenten-yl)thiopheneyl	0.47 ± 0.08
14d	5-Br-thiopheneyl	>10	**14k**	5-(1-Cyclohexen-yl)thiopheneyl	1.85 ± 0.3
14e	Benzo[b]thiophen eyl	4.85 ± 2.2	**14l**	5-(3-Furanyl)-thiopheneyl	0.52 ± 0.1
14f	5-Ph-thiopheneyl	4.22 ± 0.8	**2**	-	37.7 ± 3.6
14g	5-(2-Chloroph-enyl)thiopheneyl	1.04 ± 0.3	**3**	-	0.45 ± 0.1

Table 4. Antiproliferative Activities of compound 14j on five different DLBCL cell Lines and cytotoxicities on normal cell Lines.

Compd.	DLBCL cell lines IC_{50} (μM)					Normal cell lines IC_{50} (μM)			
	SUDHL-4	Farage	DOHH2	OCI-LY7	TOLEDO	LO2	HAF	NCM460	PNT1A
14j	0.92 ± 0.02	1.26 ± 0.06	1.21 ± 0.5	1.62 ± 0.6	3.25 ± 0.3	13.1 ± 0.6	26.4 ± 2.8	32.4 ± 0.04	8.13 ± 0.07
2	51.3 ± 2.5	33.9 ± 1.1	35.1 ± 1.9	39.0 ± 5.1	65.3 ± 2.8	>100	>100	>100	>100
3	24.3 ± 2.2	33.5 ± 0.2	47.6 ± 0.3	33.9 ± 0.7	39.5 ± 1.7	>100	>100	>100	>100

Table 5. *In Vitro* Metabolic Stability and %PPB Profiles of compound 14j.

Compd.	Human Liver Microsomal Stability				%PPB[d]
	$CL_{int(mic)}$ [a] (μL/min/mg)	$CL_{int(liver)}$ [b] (mL/min/kg)	$T_{1/2}$ [c] (min)	Remaining (T = 60 min)	human
14j	< 9.6	< 38.0	> 60	102.04%	92.4

[a]$CL_{int(mic)}$ is the intrinsic clearance; $CL_{int(mic)}$ = 0.693/half-life/mg of microsome protein per mL. [b]$CL_{int(liver)}$ = $CL_{int(mic)}$ × mg of microsomal protein/g liver weight × g of liver weight/kg body weight; mg of microsomal protein/g of liver weight: 45 mg/g; liver weight: 20 g/kg. [c]$T_{1/2}$ is half-life. [d]Plasma protein binding (PPB) studies were carried out by WuXi AppTec, Inc.

Guo, *et. al* **Figure 1**

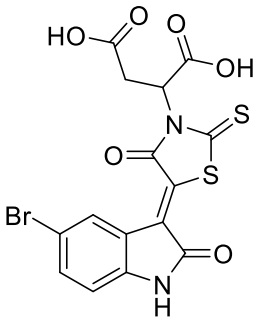

1 (79-6)

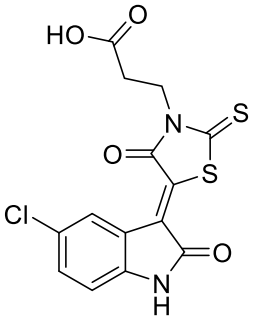

2 (FX1)

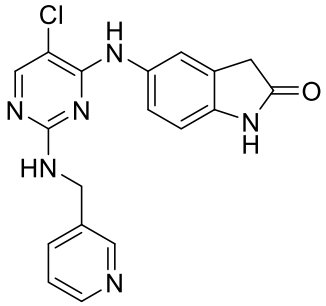

3

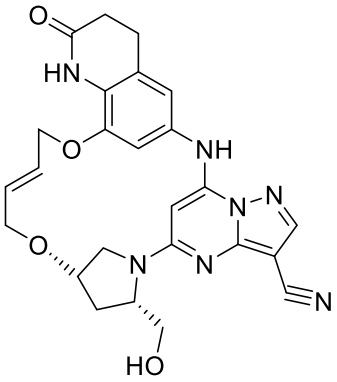

4

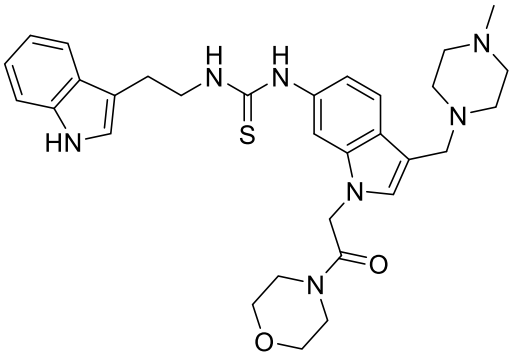

5

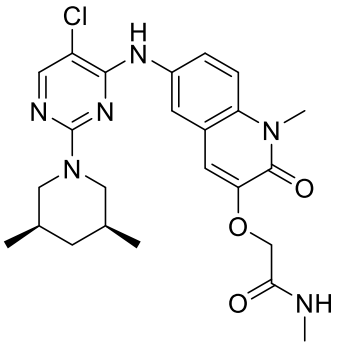

6 (BI3802)

A

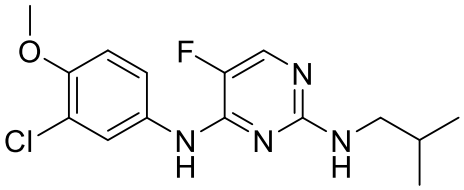

7

Hit compound

HTRF:IC_{50} = 19.4 ± 3.4 *μM*

B

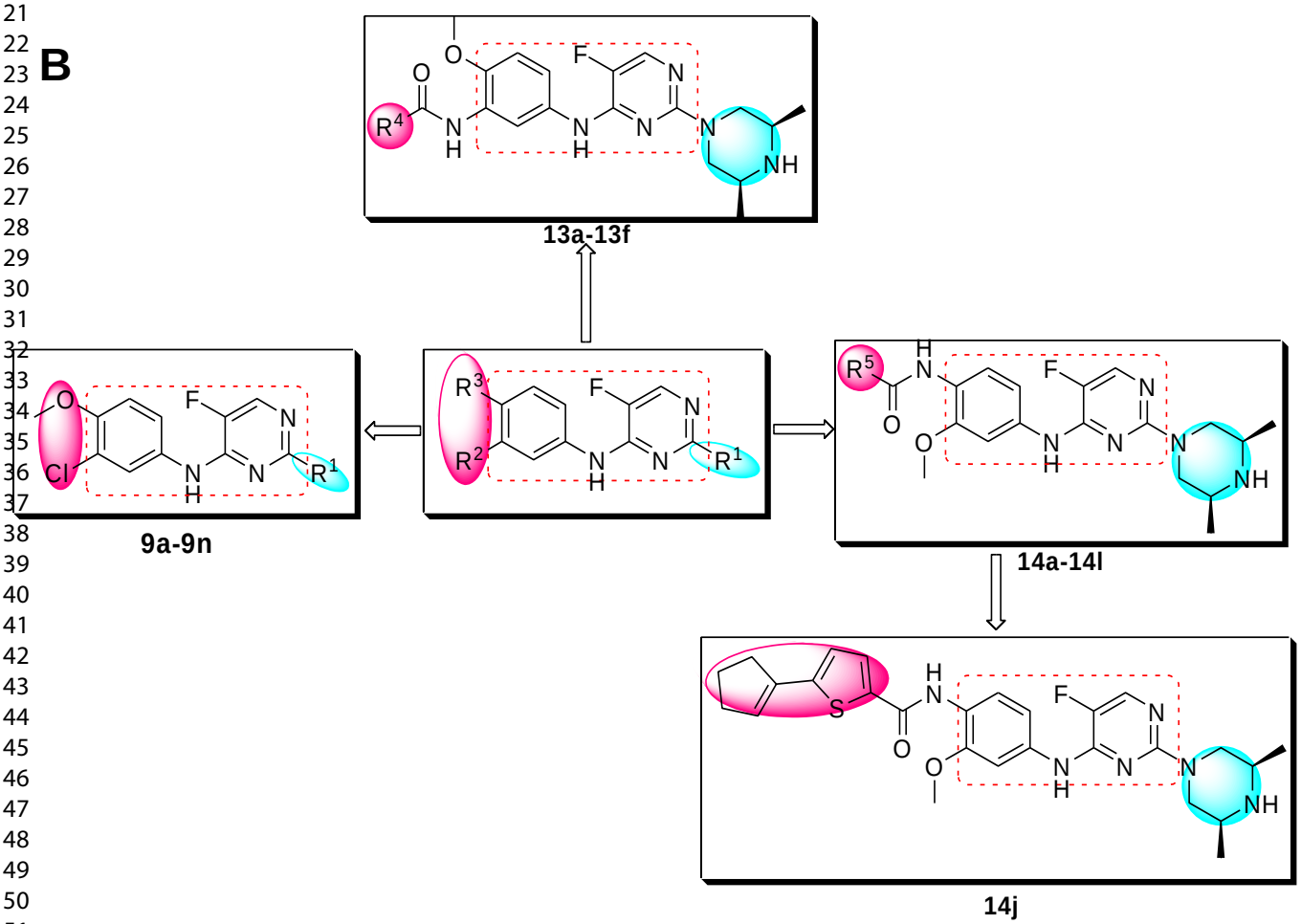

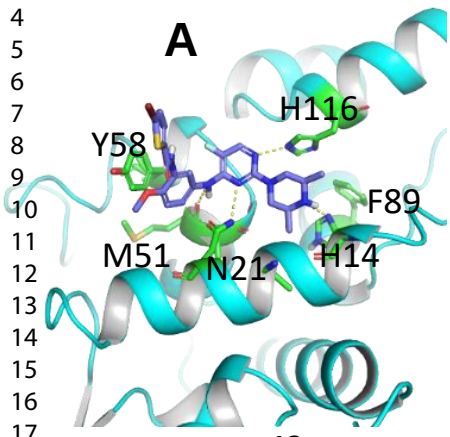

13a
Docking score: -7.19

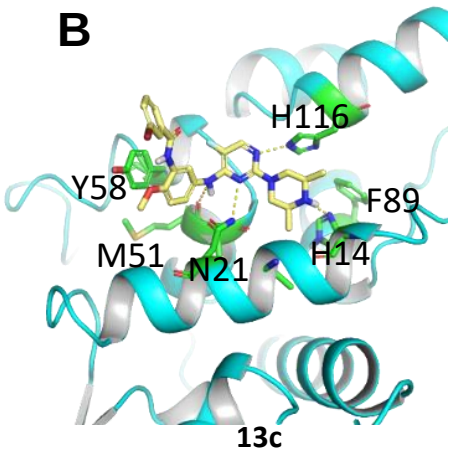

13c
Docking score: -7.85

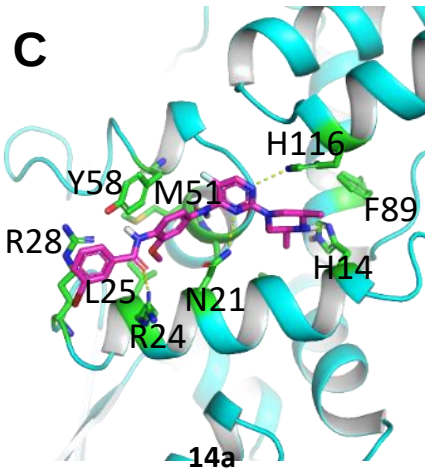

14a
Docking score: -9.69

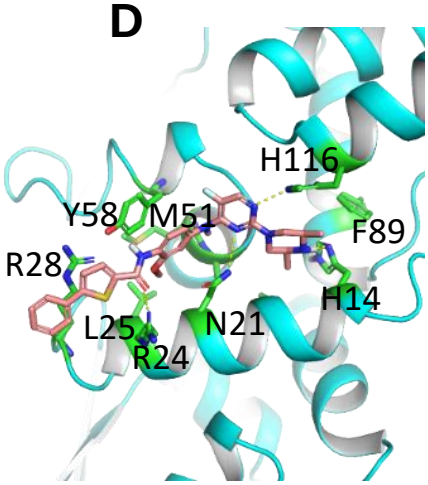

14f
Docking score: -10.41

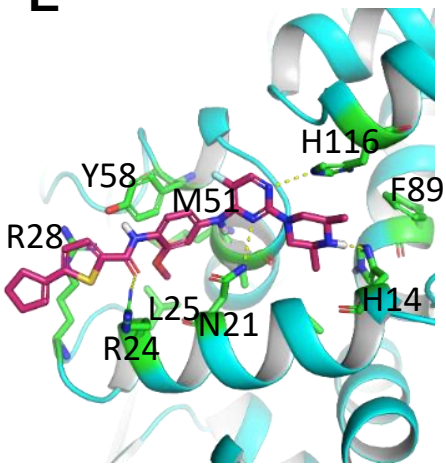

14j
Docking score: -9.96

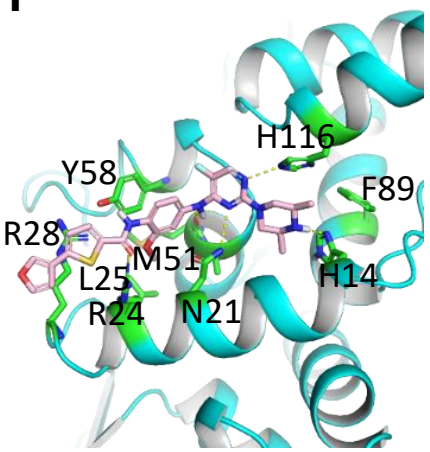

14l
Docking score: -10.76

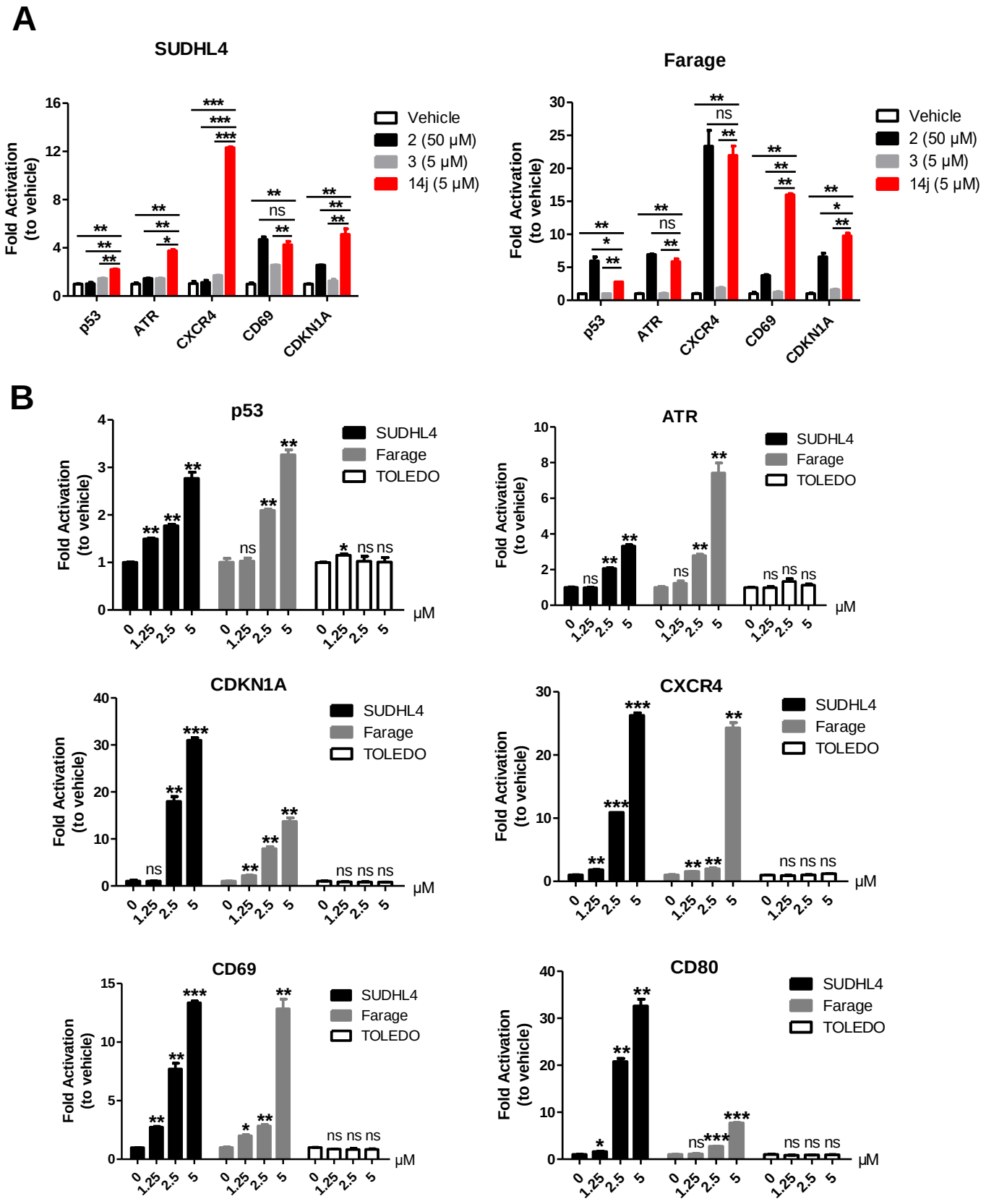
A
SUDHL4
Fold Activation (to vehicle)
Vehicle
2 (50 μM)
3 (5 μM)
14j (5 μM)
p53
ATR
CXCR4
CD69
CDKN1A
Farage
B
p53
ATR
CDKN1A
CXCR4
CD69
CD80
SUDHL4
Farage
TOLEDO
μM

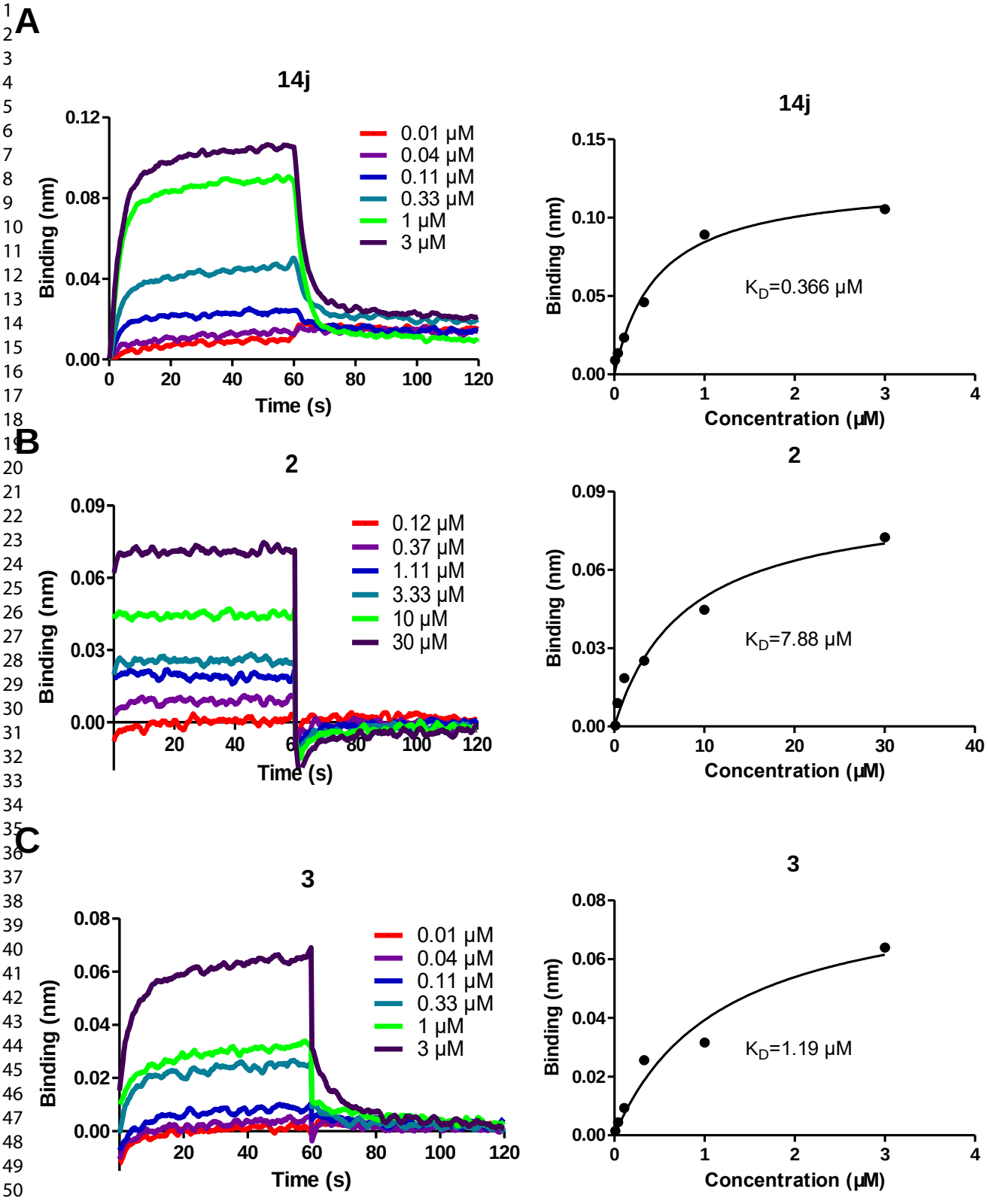
A
14j
Binding (nm)
Time (s)
0.01 μM
0.04 μM
0.11 μM
0.33 μM
1 μM
3 μM
14j
Binding (nm)
Concentration (μM)
K_D=0.366 μM
B
2
Binding (nm)
Time (s)
0.12 μM
0.37 μM
1.11 μM
3.33 μM
10 μM
30 μM
2
Binding (nm)
Concentration (μM)
K_D=7.88 μM
C
3
Binding (nm)
Time (s)
0.01 μM
0.04 μM
0.11 μM
0.33 μM
1 μM
3 μM
3
Binding (nm)
Concentration (μM)
K_D=1.19 μM

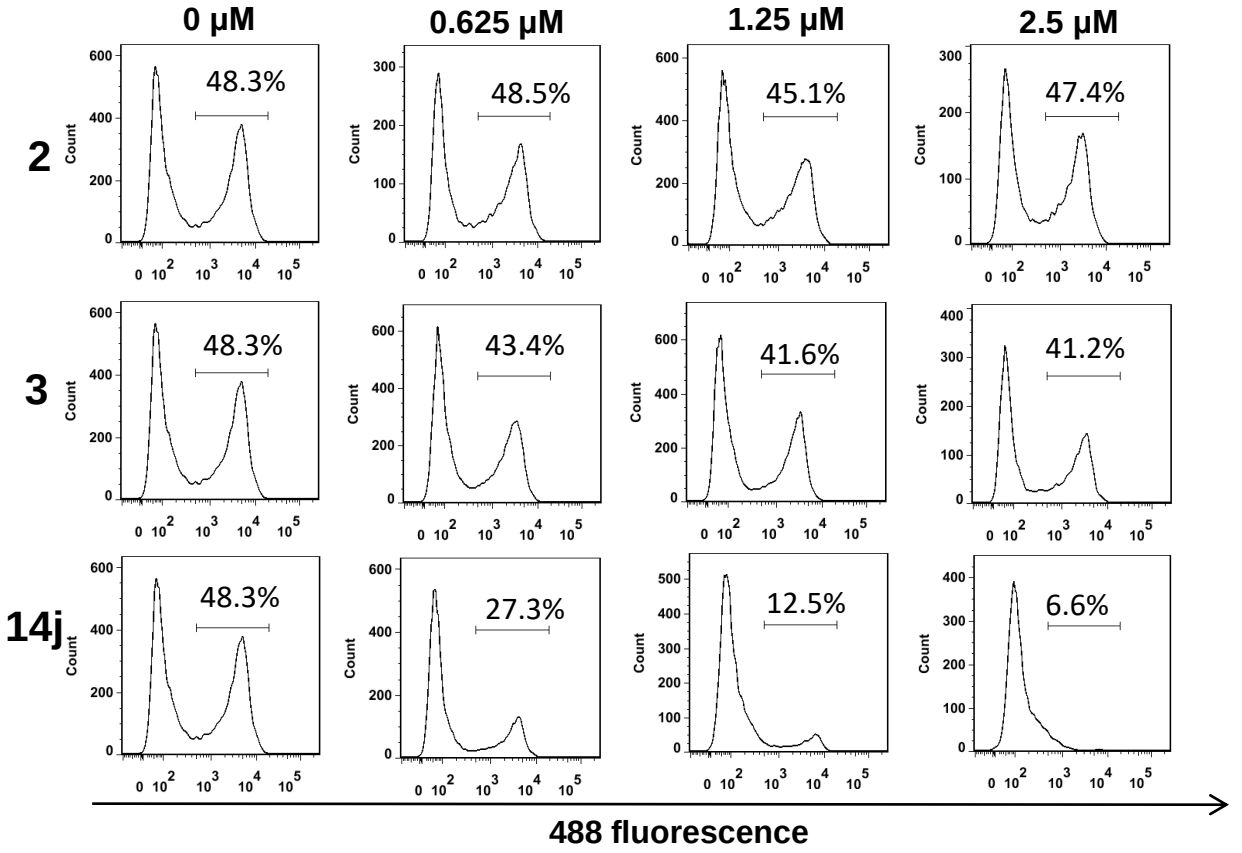
A
0 μM
0.625 μM
1.25 μM
2.5 μM
2
3
14j
48.3%
48.5%
45.1%
47.4%
48.3%
43.4%
41.6%
41.2%
48.3%
27.3%
12.5%
6.6%
Count
488 fluorescence

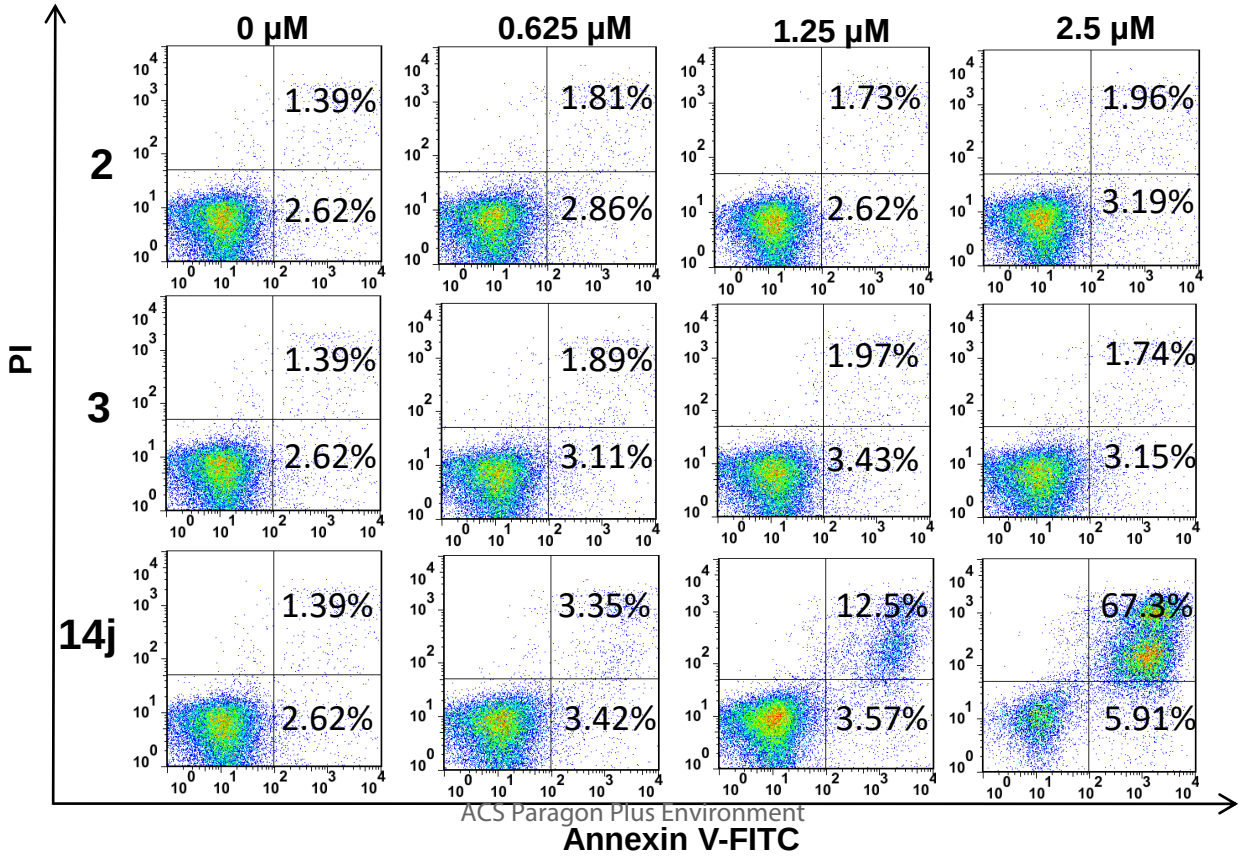
B
0 μM
0.625 μM
1.25 μM
2.5 μM
2
3
14j
1.39%
1.81%
1.73%
1.96%
2.62%
2.86%
2.62%
3.19%
1.39%
1.89%
1.97%
1.74%
2.62%
3.11%
3.43%
3.15%
1.39%
3.35%
12.5%
67.3%
2.62%
3.42%
3.57%
5.91%
PI
Annexin V-FITC

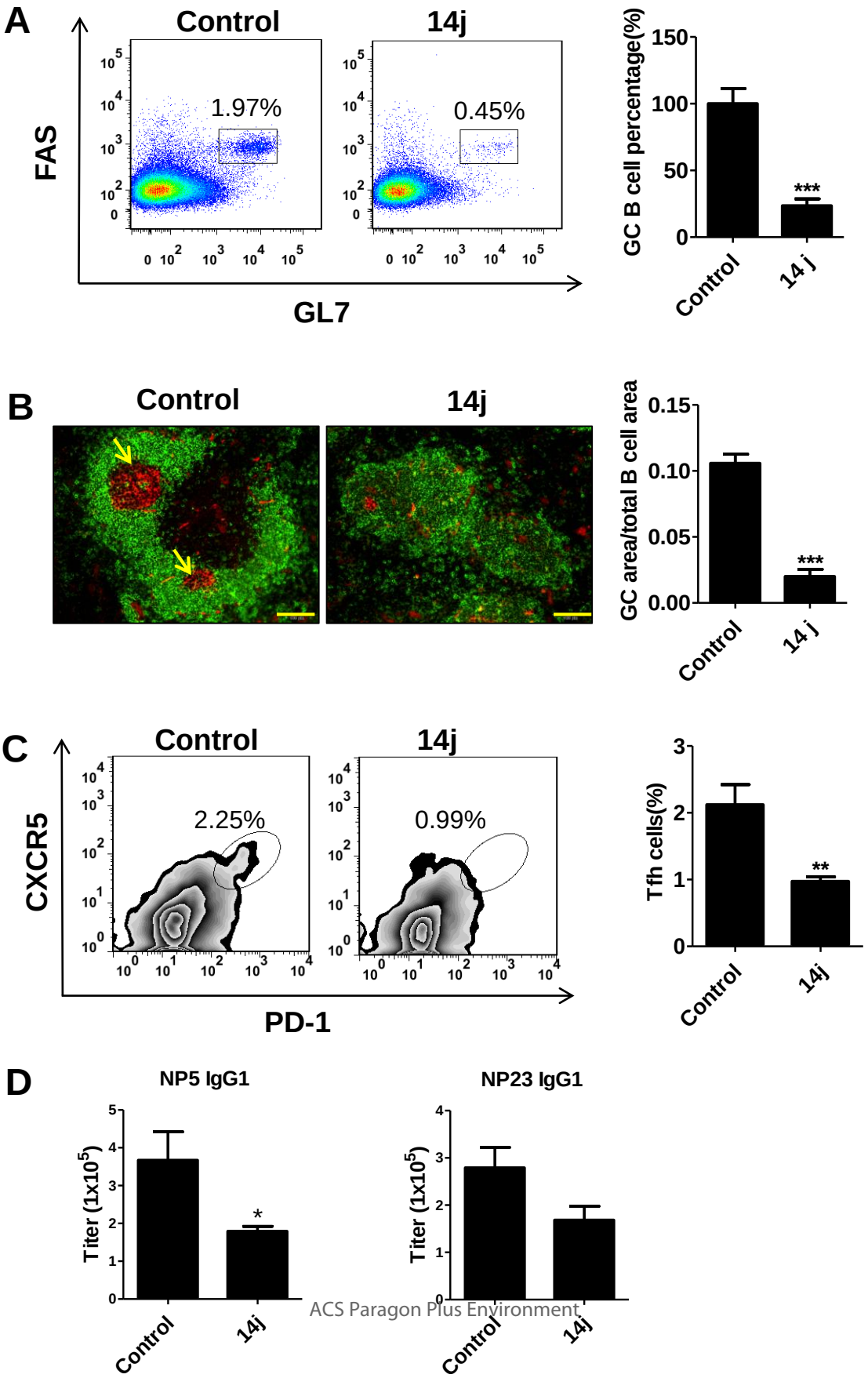

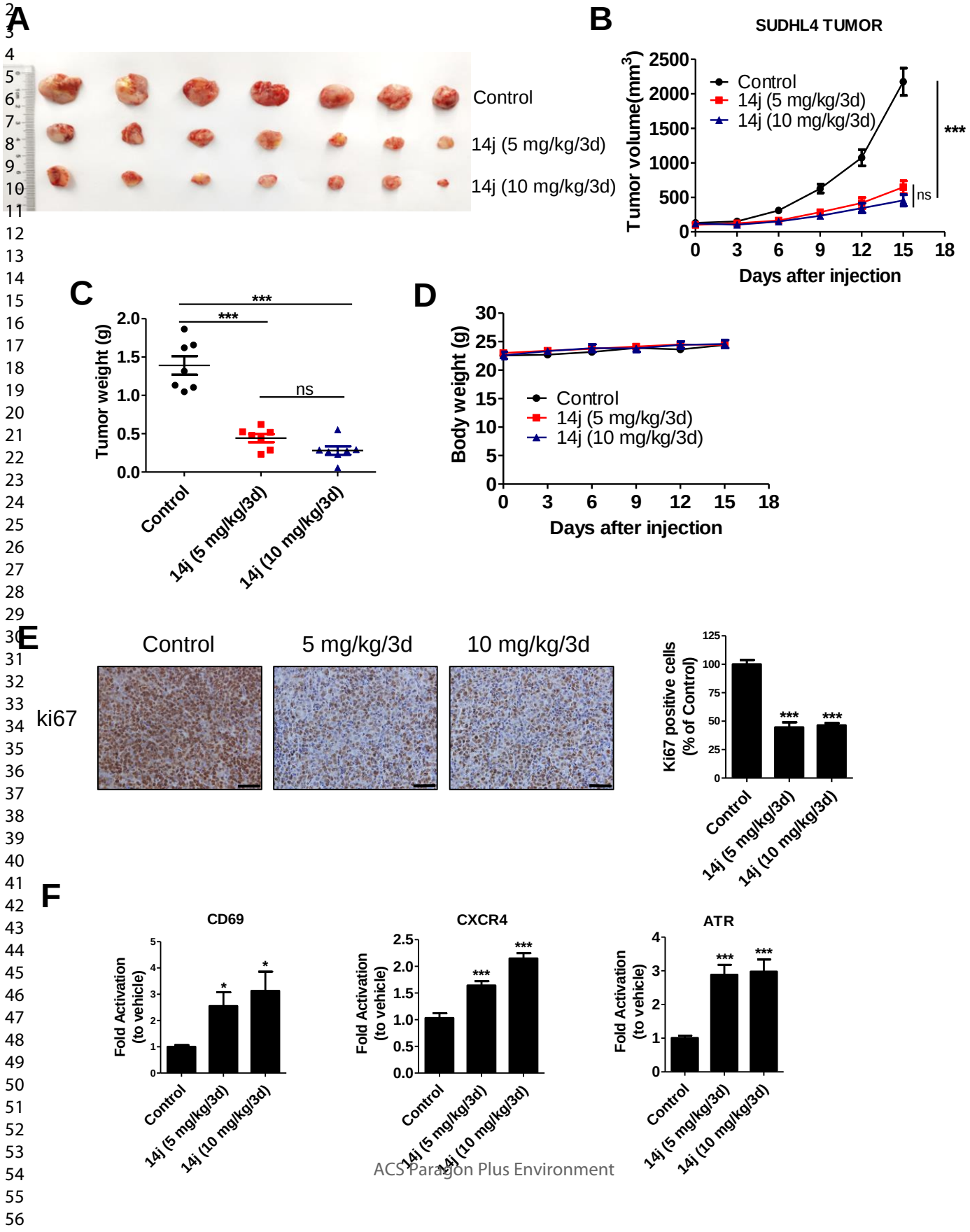
A
Control
14j (5 mg/kg/3d)
14j (10 mg/kg/3d)
B
SUDHL4 TUMOR
Tumor volume(mm3)
Control
14j (5 mg/kg/3d)
14j (10 mg/kg/3d)
***
ns
Days after injection
C
Tumor weight (g)
***
***
ns
Control
14j (5 mg/kg/3d)
14j (10 mg/kg/3d)
D
Body weight (g)
Control
14j (5 mg/kg/3d)
14j (10 mg/kg/3d)
Days after injection
E
Control
5 mg/kg/3d
10 mg/kg/3d
ki67
Ki67 positive cells (% of Control)
***
***
Control
14j (5 mg/kg/3d)
14j (10 mg/kg/3d)
F
CD69
Fold Activation (to vehicle)
*
*
Control
14j (5 mg/kg/3d)
14j (10 mg/kg/3d)
CXCR4
Fold Activation (to vehicle)
***
***
Control
14j (5 mg/kg/3d)
14j (10 mg/kg/3d)
ATR
Fold Activation (to vehicle)
***
***
Control
14j (5 mg/kg/3d)
14j (10 mg/kg/3d)

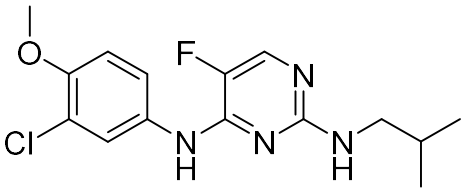

7

Hit compound

HTRF:IC_{50} = 19.4 ± 3.4 μM

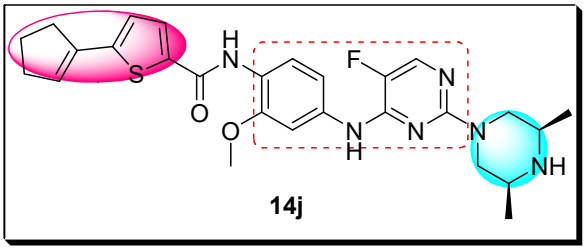

14j

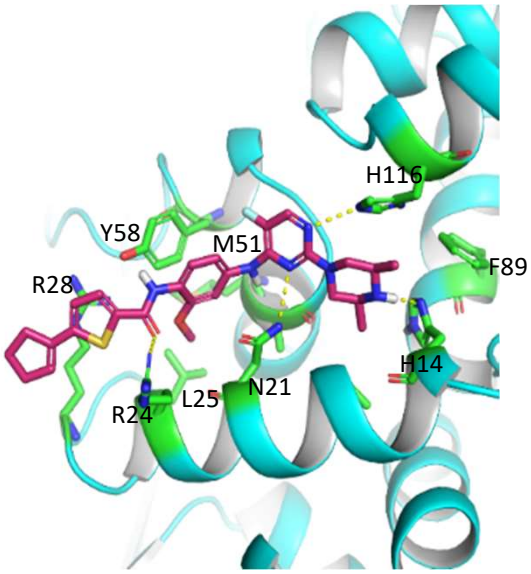

14j with BCL6 BTB